Science of the Total Environment 922 (2024) 170940

Contents lists available at ScienceDirect

Science of the Total Environment

journal homepage: www.elsevier.com/locate/scitotenv

The connection between Submarine Groundwater Discharge and seawater quality: The threat of treated wastewater injected into coastal aquifers

Aaron Alorda-Kleinglass [a,b,*], Valentí Rodellas [b,**], Marc Diego-Feliu [a], Núria Marbà [c], Carlos Morell [c], Jordi Garcia-Orellana [a,b]

[a] Institut de Ciència i Tecnologia Ambientals (ICTA), Universitat Autònoma de Barcelona, E-08193 Bellaterra, Catalonia, Spain
[b] Departament de Física, Universitat Autònoma de Barcelona, E-08193 Bellaterra, Catalonia, Spain
[c] Global Change Research Group, Institut Mediterrani d'Estudis Avançats, IMEDEA (CSIC-UIB), 07190 Esporles, Mallorca, Spain

HIGHLIGHTS

- Touristic pressure results in increased nutrient loads injected into the aquifer.
- Karstic aquifers provide preferential conduits of solutes injected into the aquifer.
- Injected wastewater effluents increase aquifer SGD-driven nutrient fluxes.
- Seagrass in Deià shows isotopic signs of anthropogenic nutrient input from SGD.

GRAPHICAL ABSTRACT

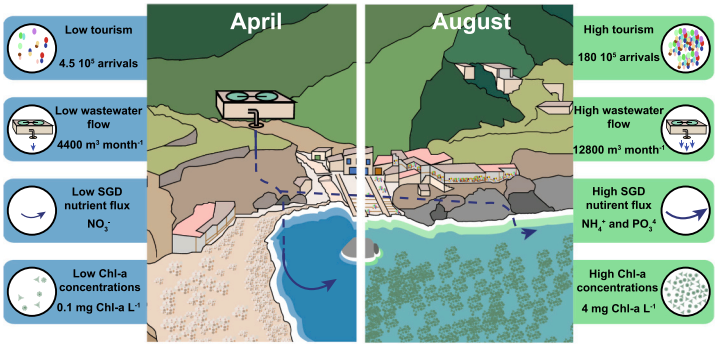

ARTICLE INFO

Editor: Jurgen Mahlknecht

Keywords:
Submarine groundwater discharge
Nutrients
Eutrophication
WWTP
Tourism

ABSTRACT

Submarine Groundwater Discharge (SGD) delivers nutrients to the coastal sea triggering phytoplankton blooms, eutrophication, and can also serve as a pathway for contaminants. Wastewater treatment plants (WWTP) including injection wells in coastal areas influence coastal aquifers and might impact the composition and magnitude of SGD fluxes. In tourist areas, wastewater treatment may be less efficient and larger in volume during high seasons, potentially impacting nutrient fluxes from SGD and exacerbating environmental impacts. This study analyzes the nutrient transfer from treated wastewater injection in karstic aquifers to the coastal sea via SGD, considering the impacts of tourism seasonality. This study is conducted in Cala Deià, a small cove in the Balearic Islands, a Mediterranean tourist destination. The findings suggest that the seasonality of tourism, leading to variations in the volume of wastewater treated in the WWTP, influences the dynamics of the coastal aquifer. This leads to increased SGD water and nutrient fluxes to the sea in summer, i.e. the peak tourist season. The measured DIN, DIP, and DSi inventories in the cove are much larger in August than in April (3, 10, and 1.5 times higher, respectively) due to higher input of nutrients in summer due to SGD impacted by the WWTP. These elevated nutrient flows can support algal blooms in the cove, compromising water quality for local swimmers and

* Correspondence to: A. Alorda-Kleinglass, Institut de Ciència i Tecnologia Ambientals (ICTA), Universitat Autònoma de Barcelona, E-08193 Bellaterra, Catalonia, Spain.
** Corresponding author.
E-mail addresses: aaron.alorda@uab.cat (A. Alorda-Kleinglass), valenti.rodellas@uab.cat (V. Rodellas).

https://doi.org/10.1016/j.scitotenv.2024.170940
Received 13 October 2023; Received in revised form 28 December 2023; Accepted 10 February 2024
Available online 14 February 2024

tourists. Indeed, in August, shoreline stations exhibited eutrophic Chl-a concentrations, with peaks reaching approximately 4 mg Chl-a L^{-1}. These elevated levels suggest the presence of an algal bloom during the survey. The anthropogenic origin of SGD-driven nutrients is traced in seawater and seagrass meadows, as evidenced by high $\partial^{15}N$ signatures indicative of polluted areas. Thus, the high pressure exerted on coastal areas by tourism activities increased the magnitude of SGD nutrient fluxes, thereby threatening coastal ecosystems and the services they provide.

1. Introduction

Submarine Groundwater Discharge (SGD) is recognized as an important contributor to the transfer of matter from land to ocean (Santos et al., 2021; Taniguchi et al., 2019) and to the well-being of coastal societies worldwide (Alorda-Kleinglass et al., 2021; Erostate et al., 2020; Moosdorf and Oehler, 2017). The magnitude and composition of SGD is strongly linked to the anthropogenic activities developed in coastal regions, such as agriculture, industry, and mining. The discharge of nutrient-rich groundwaters into coastal areas has been globally reported as a key factor in triggering high productivity of phytoplankton blooms and, in some cases eutrophication (e.g., Amato et al., 2016; Andrisoa et al., 2019; Basterretxea et al., 2010; Garcés et al., 2011; Garcia-Solsona et al., 2010; Machado and Imberger, 2014; Yoshioka et al., 2016). The process has also become recognized as an important pathway for contaminants (Dulai et al., 2016; Johannes and Hearn, 1985) across the globe (e.g. Korea, Hosono et al., 2012; USA, Wada et al., 2021; or Mexico, Kantún-Manzano et al., 2018). Among the different sources that can pollute the aquifers and influence the SGD fluxes, wastewater has been thoroughly studied during the last two decades. Either due to the leakage of septic tanks, wastewater spills, or effluents of wastewater treatment plants (WWTP), wastewater may enter the coastal aquifer and discharge into the ocean via SGD. The transfer of wastewater to the coastal aquifer and the sea has been traced by detecting fecal bacteria (Adyasari et al., 2019; Boehm et al., 2004; Knee et al., 2008; Yau et al., 2014), pharmaceuticals (McKenzie et al., 2020), pesticides (Welch et al., 2019), chemicals of emerging concern (Gutiérrez-Martín et al., 2023), changes in the nutrient levels or the nitrogen isotopic signal ($\partial^{15}N$) and algae growth (Amato et al., 2016; Andrisoa et al., 2019; Dailer et al., 2010, 2012). The consequences of polluted groundwater have been reflected in the biota, endangering coral reefs (Hernández-Terrones et al., 2015; Prouty et al., 2017), seagrass meadows (Kantún-Manzano et al., 2018), and algae for human consumption with strong cultural bonds (Dulai et al., 2023).

Most coastal WWTPs discharge their effluents into the marine environment through submarine outfalls or other superficial water bodies (e.g., rivers, ephemeral streams, or small lagoons). Alternatively, effluents of WWTP can be discharged into aquifers via injection wells, benefiting from the natural solute filtering capacity of coastal aquifers when groundwaters are transported through small aquifer pores. For instance, heterotrophic denitrification and anammox play a key role in N attenuation (Fackrell et al., 2016), whilst in karstic aquifers chemical precipitation plays a key role in P attenuation (Cable et al., 2002). However, coastal aquifers can be very permeable (e.g. volcanic or karst), and SGD can thus represent a potential pathway delivering nutrients and pollutants injected into coastal aquifers from WWTP effluents to the sea (Johannes and Hearn, 1985). The injection of WWTP into high permeable coastal aquifers has drastic consequences on coastal waters although wastewaters have been previously treated (Dailer et al., 2010; Lapointe et al., 1990). During the last decade, important advances have been made concerning the impacts of injection wells on SGD, including the quantification of anthropogenic SGD-driven nutrient fluxes (Glenn et al., 2013; Swarzenski et al., 2016), understanding the nitrogen reactions occurring in the aquifer affected by the injection of treated wastewaters (Fackrell et al., 2016), evaluating algal $\partial^{15}N$ to model nutrient loading from injection wells (Amato et al., 2020) or assessing wastewater management strategies to evaluate costs and water quality (Wada et al., 2021).

Many of those WWTPs work at their maximum capacity during the high tourism season (i.e. summer) and are often under-dimensioned for the present tourist volume (EEA, 2019). For instance, the high performance of WWTP in high season months can compromise their efficiency (i.e. capacity to reduce the nutrient load), increasing the loads of nutrients and pollutants released into the environment (Orhon et al., 1999). This is the case with many islands worldwide, where tourism has provided high incomes and socioeconomic growth (Croes, 2013). However, SGD has never been evaluated under such conditions, where tourism seasonality can influence the SGD water flow and derived nutrient fluxes, potentially causing a change in seawater quality. This study aims to evaluate the potential transference of nutrients injected into a karstic aquifer from a WWTP highly affected by tourism seasonality, to the coastal sea via SGD, and the impacts of this process on the quality of coastal waters. This study is conducted in Cala Deià (Mallorca, Illes Balears), a highly touristic small village where the effluents of the WWTP are injected into a coastal karst aquifer connected to a cove (Cala Deià).

The Illes Balears ranks among the top touristic destinations in the Mediterranean Sea, where 16 million tourists are received every year. These islands are a hotspot of high-intensity tourism, an industry accounting for ~50 % of the Balearic GDP (i.e. gross domestic product; Manera et al., 2018). Among all WWTPs in these islands, there are 32 along the coasts that either discharge into ephemeral streams, or directly inject their treated wastewater into the aquifer via injection wells. We hypothesize that in heavily fractured systems such as karstic aquifers located along the coastline of the Illes Balears, the preferential conduits can rapidly transfer the solutes injected into the aquifer from WWTP to the coastal sea, especially during the high tourism season.

2. Methodology

2.1. Study site

Cala Deià is a small cove of 80 m shore length composed of big blocks and gravels (Pujol et al., 2017), and patched with *Posidonia oceanica* meadows. The cove is located at the shores of the village of Deià, at the end of the ephemeral spring Torrent Major, on the northwest coast of the Island of Mallorca (western Mediterranean) (Fig. 1). The village is located in a valley at 300 m at the Tramuntana mountain chain, which is composed of highly karstified limestone from the Mesozoic era. Groundwater flows through this karst system emerging as natural springs along the mountainside and into the coastal ocean (Gelabert and Sàbat, 2002; Onac et al., 2005). The coastal karstified calcareous aquifer of Valldemossa-Deià covers 34.66 km^2 and is composed of a formation from the inferior Jurassic which is strongly eroded by the karst with 0.01 retention coefficient and 100 m^2 d^{-1} transmissivity (Govern de les Illes Balears, 2014). Such erosion creates large cavities inside the impermeable rock through which water travels rapidly to the ocean or flows through artisanal springs inland (Giménez et al., 2014; PUMO, 1990). The available knowledge on the springs from the area highlights their rapid response to precipitations, with increased water flows lasting only a few days after the precipitation events (Gelabert and Sàbat, 2002). At Cala Deià the bigger blooms occur during spring and summer, with 3000 and 1000 cells mL^{-1}, respectively. Those concentrations are considered to indicate moderate to low water quality conditions when those blooms

occur. The composition of those blooms is dominated by ultraflagelates and haptophytes in spring, and other ultraflagelates in summer (Puigserver et al., 2008).

Although Deià is a village of only 700 inhabitants, it constitutes one of the most important touristic hotspots of Mallorca due to its important cultural and natural heritage. The main economic activities developed in the area are based on tourism (GOIB-Observatori del treball, 2021). The climate in Deià is governed by mild winters (~9.3 °C) and hot summers (24.6 °C). It has a precipitation regime well differentiated between the wet season (autumn and spring) and dry season (summer) ranging between 600 and 800 mm y^{-1} (AEMET). The population living in the town varies seasonally as a consequence of tourism. Indeed, there is a population increase of up to 2.5 times in summer months relative to winter, due to the tourism offer (475 vacancies from hotels and ~ 700 from tourism residencies; IBESTAT, 2022; INE, 2022), resulting in high water consumption. In Deià (as well as in most of the Illes Balears), groundwaters flowing from natural springs constitute the main source of fresh water (~95 %; GOIB, 2022) for the population for most of the year (Giménez et al., 2014). Both, the demand for fresh water and the volume of wastewater increase significantly in summer because of tourism, resulting in an increase in the volume of treated wastewater in the local WWTP by a factor of ~4 (Deyà Tortella and Tirado, 2011; Garcia et al., 2022). The WWTP is located 100 m above sea level between the cove and the village. Wastewater is decanted and filtered by a bioactive film, and treated effluents are channelized to an injection well located 50 m below the station which introduces those waters into the karstic system (ABAQUA, 2022). The injection well inflows an average volume of 224 m^3 d^{-1}, with an average of 66 mg L^{-1} of nitrogen and 7 mg L^{-1} of phosphate. According to Directive 91/271/EEC the area where the treated waters are discharged, there is no maximum limit on the N or P concentrations. Despite the potential contamination of aquifer waters by injection wells associated with the wastewater treatment plant (WWTP), the inhabitants of Deià do not directly consume freshwater from the coastal part of the aquifer. Instead, the villagers consume their fresh water from the groundwaters that sprout at the different springs that are at the village of Deià (300 m asl) or from stored rainwater in cisterns. Consequently, water consumption primarily occurs from sources located above the village. During the summer months, the village faces a scarcity of freshwater as the karst system dries out. Consequently, it becomes imperative to organize cisterns to ensure the provision of essential water supplies.

2.2. Sampling methods

Two campaigns were conducted in April and August 2019 to assess the influence of WWTP effluents on the magnitude of groundwater discharge and associated nutrient fluxes to the coastal ocean. Twelve seawater stations were distributed throughout the cove plus an extra sample outside of the cove (OCN) for superficial seawater samples (~50 cm below the water surface) (Fig. 1). In August, additional deep samples (ranging between 2.5 and 4.5 m depth and sampled at ~50 cm above the seafloor) were collected at stations 5, 7, and 8. All surface and deep seawater samples were collected directly using a submersible pump. Groundwater was pumped using a submergible electric pump from a 20 cm depth hole manually excavated at the end of the Torrent Major ephemeral stream (TOR). Two superficial water samples were collected from the ephemeral stream (EPS-1 and EPS-2) and one at the WWTP from the treated wastewater effluent (Fig. 1). The ephemeral stream stations (EPS-1 and EPS-2) could not be sampled in August as both were completely dry. A submarine brackish groundwater spring, located inside the limestone fractures that directly discharged into the cove seawaters was also sampled in August (LFS, Fig. 1). This spring was not identified in April and could not be sampled.

All seawater, groundwater, ephemeral streams, and WWTP samples were measured for temperature, salinity, pH, and ORP with a multiparametric probe (YSI 670). Vertical profiles of temperature and salinity were also recorded using the multiparameter probe. In each seawater station, 60 L, 240 mL and 20 mL samples were collected to quantify Ra isotopes (^{223}Ra, ^{224}Ra, ^{226}Ra and ^{228}Ra, which are commonly used tracers of SGD; Garcia-Orellana et al., 2021), *Chl a* and dissolved nutrients (NO_x (NO_3^- + NO_2^-), NH_4^+, SiO_2, PO_4^{3-}, TDN, TDP), respectively. In August, the karstic spring (LFS) was sampled for Ra (60 L), nutrients, and *Chl a*. At the station TOR, located at the end of the ephemeral stream, which was completely dry during both seasons, 25 L of groundwater were pumped for Ra and dissolved nutrients analyses. Superficial waters from the two different ephemeral streams (EPS-1 and EPS-2) and the WWTP effluent were only sampled for physicochemical parameters and nutrients. In addition, water samples to determine nitrogen signatures (∂^{15}N), which are used as tracers to determine the N source origin, were taken from all seawater, groundwater, ephemeral streams, and WWTP samples in August. Furthermore, three different replicates of leaf shoots were taken from the seagrass meadow of *P. oceanica* at stations 7, 10, 12, and OCN to determine ∂^{15}N.

Seawater and groundwater samples collected for Ra isotopes were

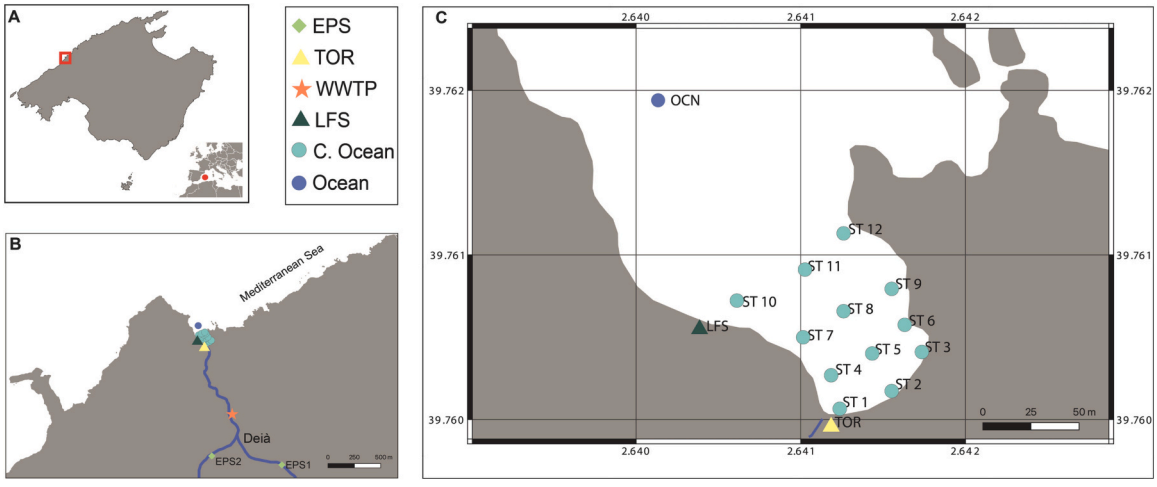

Fig. 1. The study site is located at the western Mediterranean basin, at the N-W side of the island of Mallorca (Illes Balears). A) Location of the sampling site on the island of Mallorca. B) The locations of an ephemeral streams draining to the cove (blue line), freshwater springs that nourish the stream (green diamond) and the injection well of the WWTP (orange star) are represented. Samples were collected from the WWTP, the two freshwater springs, SGD endmembers, including the end of the Torrent Major (TOR; yellow triangle) and a freshwater spring at the western side of the cove (LFS; green triangle). Coastal seawater stations and the offshore station are represented with light and dark blue circles, respectively. C) Detailed location of the seawater stations, Torrent Major and karstic spring.

filtered (<1 L min^{-1}) through 20 g of dry acrylic fibers impregnated with MnO_2 to adsorb Ra isotopes (Moore and Reid, 1973). Samples for *Chl a* were filtered through GF/F filters (0.7 μm) and the filters were frozen for further analysis. Nutrient and $\partial^{15}N$ samples were filtered through nylon syringe filters (φ 0.45 μm) and stored in 10 mL polyethylene vials, which were immediately refrigerated and then frozen until analysis. Leaf shoots were stored in zip-lock plastic bags and refrigerated until arriving at the lab where they were dried at 60 °C for 48 h.

2.3. Analytical methods

After filtration, Mn-fibers were rinsed with Ra-free water to remove particles or salt that could interfere during measurement (Sun and Torgersen, 1998). Short-lived Ra isotopes (^{223}Ra and ^{224}Ra) were counted with a Radium Delayed Coincidence Counter (RaDeCC; Moore and Arnold, 1996). Ra-224 was quantified following the criteria and recommendations described by Diego-Feliu et al. (2020) with uncertainties calculated according to Garcia-Solsona et al. (2008). Ra-224 activities were corrected for ^{228}Th and ^{223}Ra was not quantified due to the significant interference between channels (cross talk) from the ^{224}Ra (Diego-Feliu et al., 2020). For the quantification of long-lived Ra isotopes (^{226}Ra and ^{228}Ra), Mn-fibers were incinerated at 820 °C for 16 h and counted by gamma spectrometry using a well-type HPGe detector after aging the samples for at least 21 days. Ra-228 and ^{226}Ra activities were determined through the photopeaks of ^{228}Ac at 911 keV and ^{214}Pb at 351 keV, respectively.

Dissolved NO_3^-, NO_2^-, NH_4^+ (DIN; $NO_3^- + NO_2^- + NH_4^+$), PO_4^{3-} (DIP), SiO_2 (DSi), TDN, and TDP were determined with an Autoanalyzer AA3 HR (Seal Analytica) using colorimetric techniques (Grasshoff, 1983) at the ICM-CSIC. The detection limits for NO_x, NO_2^-, NH_4^+, PO_4^{3-}, TDN, and TDP in the lowest range (MDL) of the analysis were 0.006, 0.003, 0.003, 0.010, 0.071 and 0.032 μM, respectively. The lowest detectable range for NO_x, NO_2^-, NH_4^+, PO_4^{3-}, TDN and TDP of the analysis were 0–4.0, 0–2.0, 0–5.0, 0–4.8, 0–71.0 and 0–22.6 μM, respectively. With a coefficient variance of 0.13 %, 0.20 %, 0.30 %, 0.20 %, 0.30 % and 0.50 %, respectively.

Water samples for $\partial^{15}N$ were defrosted and analyzed following the hypobromite method by (Zhang et al., 2007) in a Thermo Finnigan PreCon (Thermo Scientific) couplet to an isotope-ratio mass spectrometer IRMS (Finnigan MAT-253) at the MAiMA-UB. Analytical reproducibility of the reported ∂ values, based on sample replicates, was better than ±0.3 ‰ for $\partial^{15}N$.

Dried *P. oceanica* leaves were grounded (Fourqurean et al., 2007), and $\partial^{15}N$ was analyzed using standard elemental analyzer isotope ratio mass spectrometer (EA-IRMS) at the Universidad de la Coruña (Spain). The EA-IRMS was used to combust the organic material and to reduce the formed gases into N_2, which was measured on a Finnigan MAT Delta C IRMS in a continuous flow mode. Analytical reproducibility of the reported $\partial^{15}N$ values for seagrass leaves, based on sample replicates, was better than ±0.2 ‰ for $\partial^{15}N$.

The sample isotopic ratios (R) are reported in the standard delta notation (‰):

$$\partial^{15}N\ (‰) = \left[\left(\frac{R_{sample}}{R_{standard}}\right) - 1\right] \cdot 1000 \quad (1)$$

where R_{sample} and $R_{standard}$ refer to the isotopic ratio of the sample and the standard, respectively. These R are presented concerning the international standards of atmospheric nitrogen (AIR, N_2).

3. Results

3.1. Groundwater, ephemeral stream, and WWTP

Groundwater from the final part of the ephemeral stream (TOR) presented similar salinities in April and August with values of 9.3 and 9.1, respectively. Waters from the upstream part of the ephemeral stream (EPS1 and EPS2), which was only flowing in April, had salinities of <1 and the WWTP effluent waters had salinities of 1.0 and 1.8 in April and August, respectively. Groundwater from the karstic spring (LFS), which was only flowing in August, had salinities of 29, mainly because this sample was collected below surface seawater and has already undergone mixing with seawater.

Radium activities presented important differences between April and August (see supporting information (S1)). ^{224}Ra in the ephemeral stream (TOR) were three times higher in April (96 ± 9 dpm 100 L^{-1}) than in August (33 ± 4 dpm 100 L^{-1}). However, concentrations of long-lived Ra isotopes were similar in April (41 ± 1 and 27 ± 2 dpm 100 L^{-1} for ^{226}Ra and ^{228}Ra, respectively) and August (30 ± 3 and 24 ± 3 dpm 100 L^{-1} for ^{226}Ra and ^{228}Ra, respectively). Groundwaters from the karstic spring (LFS) had much higher concentrations for all Ra isotopes compared to TOR (160 ± 4, 57 ± 5 and 98 ± 8 dpm 100 L^{-1} for ^{224}Ra, ^{226}Ra, and ^{228}Ra, respectively). It should also be noticed that groundwaters from TOR and LFS have a similar and low $^{224}Ra/^{228}Ra$ ratio (1.4 ± 0.2 and 1.6 ± 0.2 for TOR and LFS, respectively), suggesting that groundwater transit time through the aquifer is long enough to reach equilibrium for these isotopes (Diego-Feliu et al., 2021; Garcia-Orellana et al., 2021).

Groundwater nutrient concentrations and speciation also presented important differences between April and August (see supporting information (S2)). Regarding groundwater from the end of the ephemeral stream (TOR), DIN concentrations were significantly higher in April than in August (110 and 16 μmol L^{-1}, respectively). DIN was mainly composed of NO_3^- (66 %) in April, whilst NH_4^+ (95 %) was the main component of DIN in August. Similarly, PO_4^{3-} concentrations were one order of magnitude lower in April than in August (0.78 and 11 μmol L^{-1}, respectively). Focusing on August, DIN and DIP concentrations measured in TOR (0.5 μmol L^{-1}, 0.35 μmol L^{-1}, and 16 μmol L^{-1} for NO_3^-, NO_2^- and NH_4^+ respectively, and 10 μmol L^{-1} for PO_4^{3-}) were lower than those measured in the karstic spring (LFS) (1.5 μmol L^{-1}, 0.52 μmol L^{-1}, and 240 μmol L^{-1} for NO_3^-, NO_2^- and NH_4^+, respectively and 18 μmol L^{-1} for PO_4^{3-}). DIN concentrations were relatively low in both surface waters from the stream (39 and 31 μmol L^{-1} for EPS-1 and EPS-2, respectively) and were mainly composed of NO_3^- (90 % and 97 %, respectively). The highest concentration of nitrogen and phosphorous was measured in the WWTP. Concentrations of DIN in the WWTP effluent followed a similar pattern to that of TOR and LFS, both in concentration and speciation. Significantly higher DIN concentrations were measured in August (243 μmol L^{-1}) relative to April (110 μmol L^{-1}); the main component of DIN was NO_3^- in April and NH_4^+ in August (77 % and 75 %, respectively). PO_4^{3-} concentrations in both springs were negligible (< 0.05 μmol L^{-1}) and the WWTP had similar concentrations during April and August (73 and 66 μmol L^{-1}, respectively). Concentrations for SiO_2 were comparable in TOR (9.1 μmol L^{-1} and 16.5 μmol L^{-1} for April and August, respectively) and LFS (17.4 μmol L^{-1}), but they were significantly higher in EPS-1, EPS-2, and WWTP (48, 31, 40 μmol L^{-1}, respectively).

3.2. Seawater

Salinities inside the cove ranged from 36.7 to 38.4 in April and were slightly fresher in August, ranging from 36.2 to 38.0 (offshore salinities of 38.4 and 38.1, respectively). During both seasons, seawater salinities were fresher on the western side of the cove. The fresher salinities were reported in samples collected in front of the end of the ephemeral stream (TOR) in April and in front of the groundwater spring (LFS) in August (Fig. 2). However, during August there was a clear stratification, with a fresher layer of ~0.7 m at the surface on the western half of the cove (see supporting information S3).

Radium concentrations in coastal waters were higher than in open seawater (Fig. 2), except for ^{226}Ra in April, most likely reflecting Ra inputs from groundwater at the stations nearer to TOR and LFS. In April, ^{224}Ra ranged from 1 to 14 dpm 100 L^{-1} inside Cala Deià and showed a

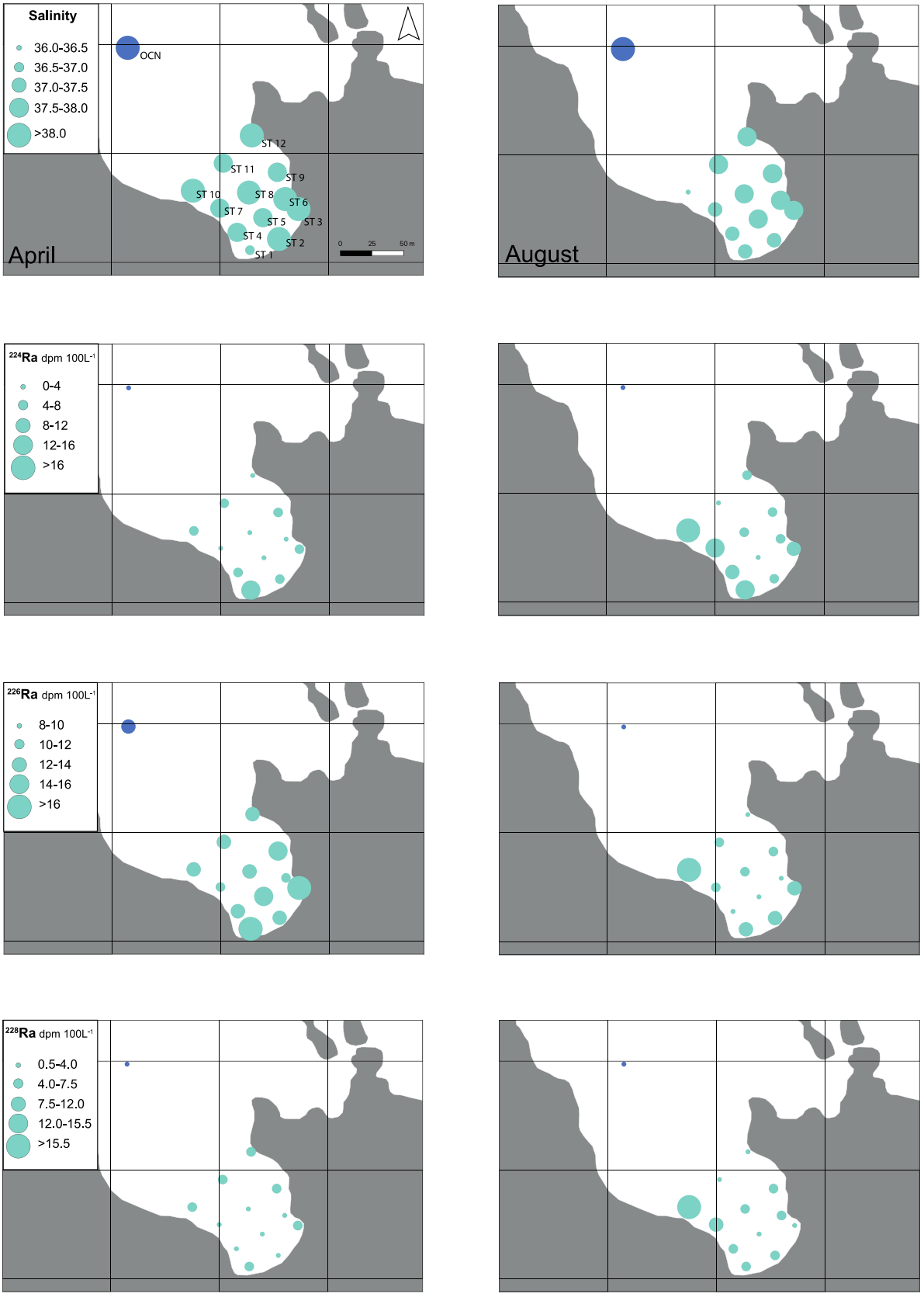

Fig. 2. Distribution of salinity and Ra isotope activities during April and August sampling campaigns. The size of the circle scales with salinity and Ra activities.

downward offshore gradient from ST1 to the exterior of the cove. However, ^{226}Ra (ranging from 11.8 to 19.6 dpm 100 L^{-1}) and ^{228}Ra (ranging from 0.8 to 6.2 dpm 100 L^{-1}) had a scattered distribution along the cove, although the highest activities were always measured at ST1 (19.6 ± 0.6 dpm 100 L^{-1} and 6.2 ± 0.9 dpm 100 L^{-1}, respectively). In August, seawater activities of ^{224}Ra and ^{228}Ra (ranging from 1.2 to 33 dpm 100 L^{-1} and from 1.8 to 21 dpm 100 L^{-1}, respectively) were higher compared to those measured in April and showed a clear gradient starting from the western side towards the exterior of the cove (Fig. 2). Contrarily, ^{226}Ra had relatively low activities (ranging from 9.5 to 19 dpm 100 L^{-1}) presenting a scattered distribution, except for sample ST10 (19 dpm 100 L^{-1}), which is the nearest sample to the LFS.

There is a clear relationship between nutrient concentrations and salinity in coastal waters, with higher concentrations measured in sites with fresher salinities and lower concentrations at offshore stations (Fig. 3). Nutrient concentrations and speciation varied significantly between seasons. In April there was a clear gradient of NO_3^- (0.4–7.6 μmol L^{-1}) on the western side of the cove towards the open ocean (0.4 μmol L^{-1}), with maximum values (7.6 μmol L^{-1}) at the nearest sample to the ephemeral stream (ST 1). Ammonia (NH_4^+ 0.2–7.4 μmol L^{-1}) did not show such a clear gradient and had similar concentrations to NO_3^- around the cove (see Fig. 4). There was no significant gradient or enrichment for NO_2^- relative to open ocean (0.02–0.15 μmol L^{-1}). Concentrations of SiO_2 (0.8–5.3 μmol L^{-1}) and PO_4^{3-} (0.003–0.430 μmol L^{-1}) in April also presented a moderate gradient offshore, although the concertation differences were not as large as for NO_3^-. Concentrations of NH_4^+ and PO_4^{3-} in seawater were one order of magnitude higher in August than in April (Fig. 4). There was a marked gradient of NH_4^+ (1–56 μmol L^{-1}) in August along the cove, from high levels on the western and central areas of the cove, especially ST10, towards the open ocean (Fig. 3). The other nitrogen species concentrations (NO_2^- (0.02–0.17 μmol L^{-1}) and NO_3^- (0.3–1.3 μmol L^{-1})) were relatively low and did not show any clear gradient or pattern. Although SiO_2 (0.6–6.8 μmol L^{-1}) and PO_4^{3-} (0.03–4.80 μmol L^{-1}) were also enriched in nearshore seawater (especially at ST10) relative to open ocean values, they did not show the same clear trends as observed for NH_4^+ (Fig. 3).

Chlorophyll *a* (Chl *a*) concentrations in April were low (0.03–0.11 mg Chl *a* L^{-1}) with maximum concentrations at the nearshore seawater samples (ST1, 2 and 3). During August, the concentrations ranged between 0.05 and 4.46 mg Chl *a* L^{-1} with maximum values of 4.5, 3.6, 1.5, and 1.7 mg L^{-1} at the shallowest stations ST 1, 2, 3, and 4, respectively.

Most water samples had low DIN concentrations that prevented the determination of ∂^{15}N. Isotopic signatures of ∂^{15}N for the WWTP effluent, the karstic spring (LFS), and the station in front of the spring (ST10) were 15.2 ‰, 10.3 ‰, and 8.7 ‰, respectively. *Posidonia oceanica* leaves inside the cove presented a mean ∂^{15}N value of 4.1 ± 1.5 ‰ (n = 4) and a maximum of 6.2 ‰, and samples collected in meadows farther from the coast (ST-OCN) presented the highest ∂^{15}N value (7.2 ‰).

4. Discussion

4.1. Water flows driven by SGD

To evaluate the role of SGD in Cala Deià as a conveyor of nutrients from a WWTP, which injects its effluents into the coastal karstic aquifer, it is necessary to identify all sources of SGD into the cove. According to the geological karst formation of the cove and the distribution of salinities, nutrients, and Ra isotopes in the cove, we have identified two predominant discharge point sources: subterranean flows from the stream (TOR) and inputs from the karstic spring (LFS), the latter only inflowing to the cove in summer.

Radium isotopes are one of the most widely used tracers to estimate SGD water flows and associated nutrient fluxes (Garcia-Orellana et al., 2021; Taniguchi et al., 2019) and groundwater origins (Diego-Feliu et al., 2022; Michael et al., 2011; Rodellas et al., 2017). The use of these isotopes to assess the role of SGD in Cala Deià requires constraining all sources and sinks of these radionuclides in and out of the cove. A mass balance of the long-lived ^{228}Ra isotope has been used to assess SGD and associated nutrient fluxes in the Cala Deià. Notice that we have preferably used ^{228}Ra because (1) coastal seawater is enriched in this radionuclide relative to the open ocean, and (2) this radionuclide is indicative of relatively long pathways and groundwater transit times as those occurring at the study site (e.g., terrestrial groundwater discharge through karstic springs). Thus, we avoid using the short-live ^{224}Ra since it may include other short-scale processes (e.g., porewater exchange) which may play a minor role in transporting nutrients into the coastal ocean in this system.

To estimate the flow of SGD a ^{228}Ra box model was used assuming steady-state conditions (see Eqs. (2) and (3)).

$$F_{^{228}Ra-SGD} + F_{sed} + F_{atm} + F_{stream} = \frac{\left(^{228}Ra_{cw-ex}\right)\cdot V}{\tau_r} + \left[\lambda\cdot^{228}Ra_{cw}\cdot V\right] \quad (2)$$

In Eq. (2), the terms found on the left represent the inputs of Ra into the system, and those on the right the outputs. On the left, $F_{^{228}Ra}$ is the ^{228}Ra flux from SGD (dpm·d^{-1}), F_{sed} is the ^{228}Ra flux from the sediments (dpm·d^{-1}), F_{atm} is the ^{228}Ra flux from the atmospheric deposition (dpm·d^{-1}), and F_{stream} the ^{228}Ra flux from superficial waters (dpm·d^{-1}). On the right we account for the Ra losses due to radioactive decay $\left[\lambda\cdot^{228}Ra_{cw}\cdot V\right]$, which depends on the decay constant of ^{228}Ra (λ; d^{-1}), the activity of ^{228}Ra in the system ($^{228}Ra_{cw}$; dpm m^{-3}) and the volume of the system (V; m^3), and the offshore outputs ($\frac{\left(^{228}Ra_{cw-ex}\right)\cdot V}{\tau_r}$), which depend on the Ra excess in the cove relative to offshore concentrations ($^{228}Ra_{cw-ex}$; dpm m^{-3}), the volume of the box (V; m^3) and the flushing time of the isotopes in coastal waters (τ_r; d). The SGD water flow (F_{SGD}; $m^3\cdot d^{-1}$) can be obtained by dividing the $F_{^{228}Ra\ SGD}$ by the ^{228}Ra activity in groundwaters discharging to the system, i.e. the SGD endmember ($^{228}Ra_{SGD}$; dpm m^{-3}) (Eq. (3)).

$$F_{SGD} = \frac{F_{^{228}Ra\ SGD}}{^{228}Ra_{SGD}} \quad (3)$$

During both samplings, the ephemeral stream was completely dry, and precipitations had not occurred during the previous 15 days (Fig. 5). No other water inputs are known or could be identified in the cove during the study. Thus, inputs of ^{228}Ra from streams can be neglected. The flux from the sediments can also be neglected since the deeper samples on the different samplings did not show a clear enrichment of Ra in comparison to the surface samples. In addition, the Ra sediment flux was also discarded due to the composition of the seabed, formed by stones and coarse-grain sands, which can be considered to have low U/Th content (Luek and Beck, 2014) and often represent a minor contribution of Ra (<10 %) compared to total Ra inputs, particularly for long-lived Ra isotopes such as ^{228}Ra (Beck et al., 2007; Garcia-Orellana et al., 2014; Rodellas et al., 2015b). The coastal waters experience a negligible impact from tides, given that the tidal range is below 0.3 m. The atmospheric input was neglected as a Ra source because its contribution in small-scale study sites is often not higher than 1 % (Garcia-Orellana et al., 2021). Inputs of Ra in the cove are thus only dependent on the supply via SGD, which is mainly inflowing to the cove through the karstic spring (LFS) only discharging in summer, and subterranean flows from the stream area (TOR). This assumption is indeed consistent with the highest activities of Ra isotopes observed in near-shore areas close to the ephemeral stream and the limestone fracture.

The volume of the system V was obtained from the area of the cove (constrained by the 12 stations: 10,200 m^2) and a depth determined by the water stratification in summer (0.7 m), resulting in a more conservative result. As a proxy of flushing times in the cove, we have used the activity ratios (AR) of ^{224}Ra/^{228}Ra to estimate the apparent water age (τ_r). Following (Moore, 2000), we estimated the τ_r using Eq. (4). We used ^{224}Ra since it is the isotope with the shortest half-live (3.6 d) and thus best suited for estimating short temporal scales as those expected in

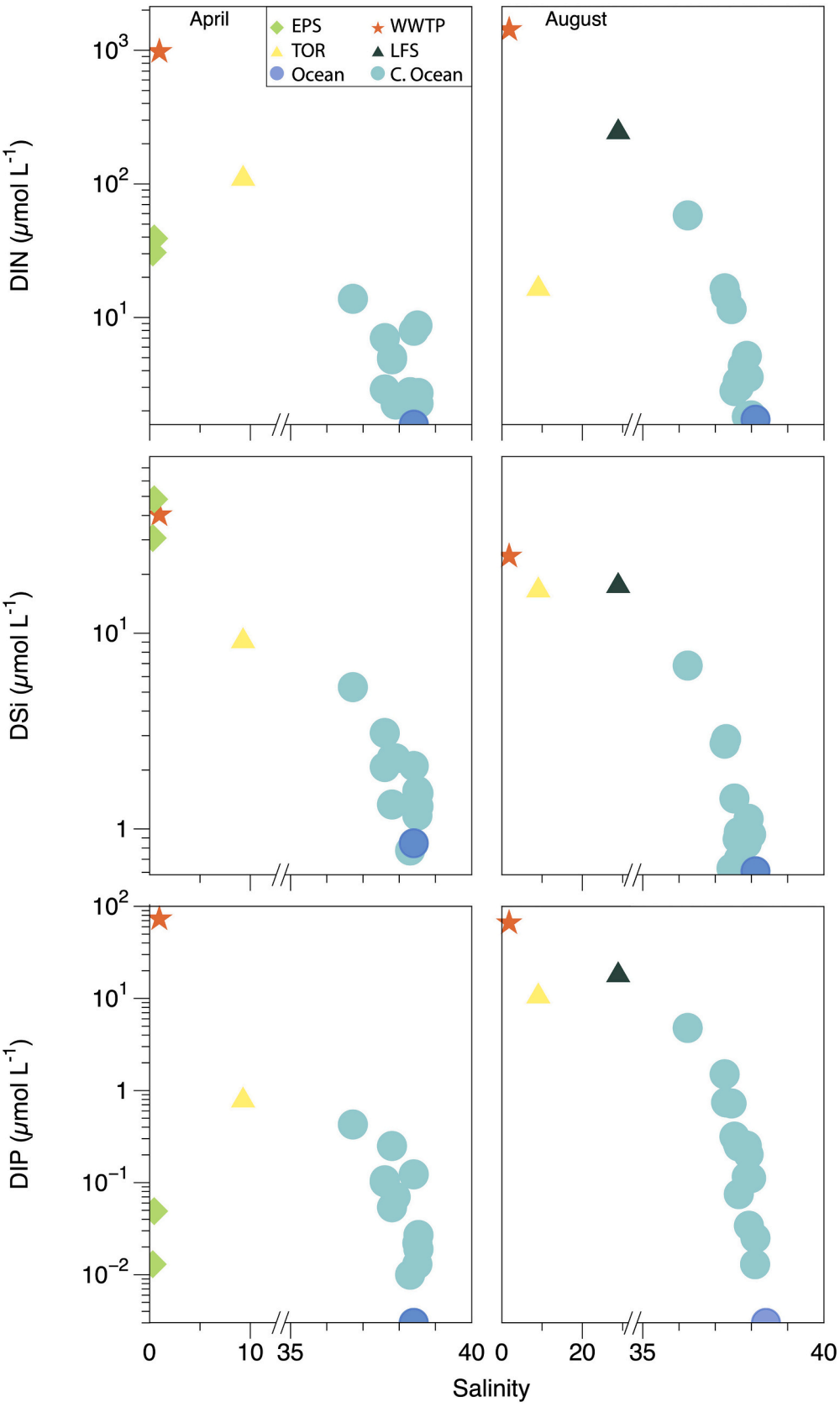

Fig. 3. Nutrient concentrations along the salinity gradient in the study site. Samples correspond to surface water from the ephemeral stream (EPS-1 and EPS-2) (April), groundwater from the end of the ephemeral stream (TOR), groundwater discharge from the limestone fracture located at the western side of the cove (LFS), water from the injection well (WWTP), coastal seawater stations and the offshore station.

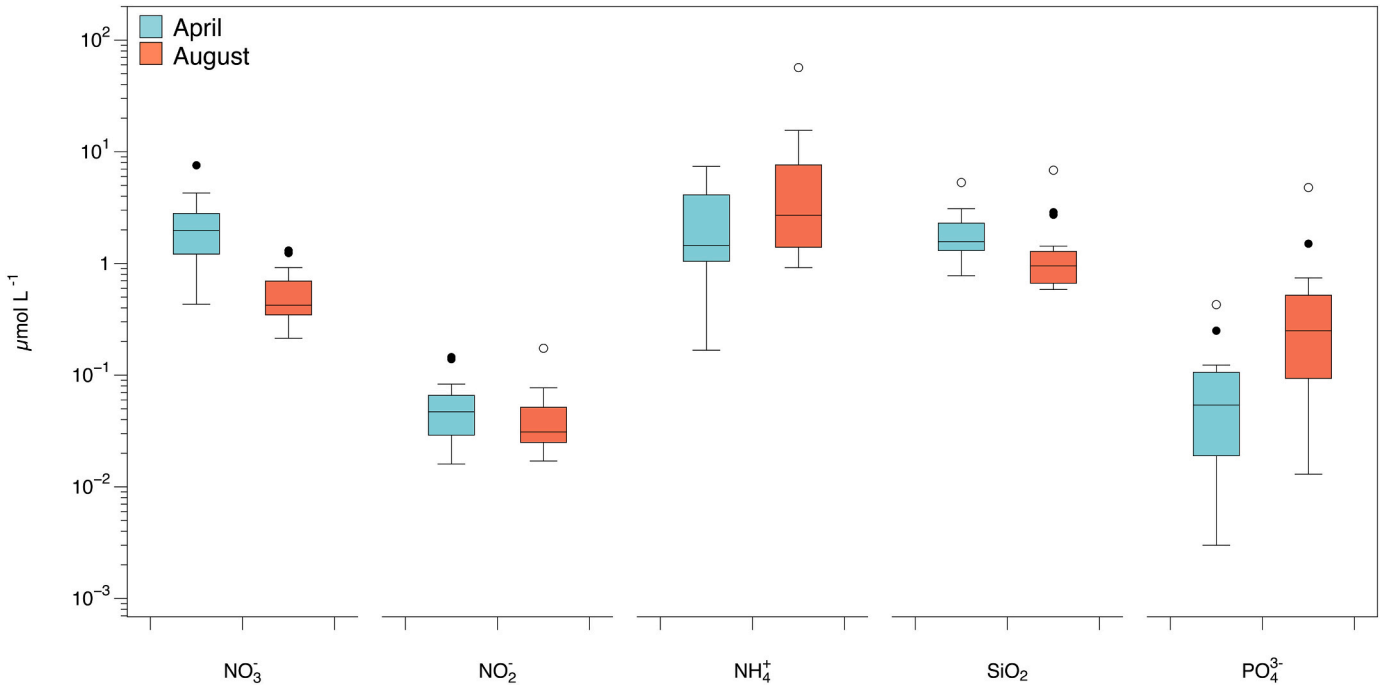

Fig. 4. Dissolved inorganic nutrient concentrations in coastal waters during April and August. Whiskers correspond to the standard deviation, black dots correspond to outliers up to 90th percentile, white dots correspond to outliers in the 90th percentile, the line inside the boxplot corresponds to the median (or second quartile).

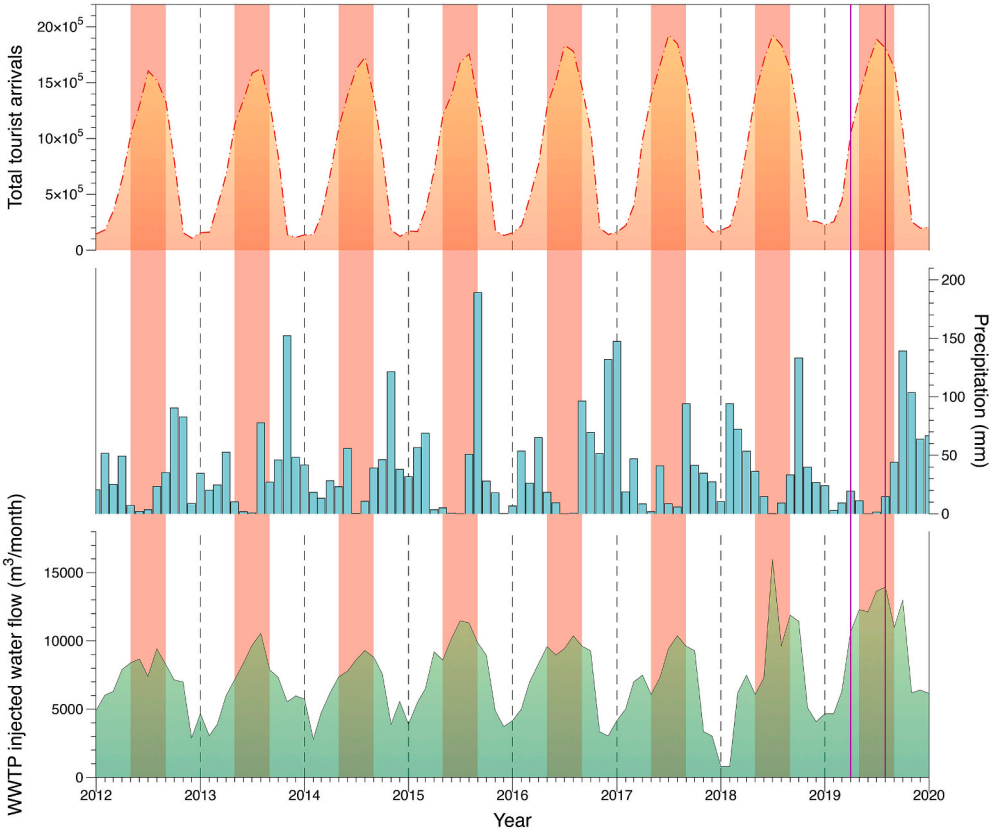

Fig. 5. Time evolution (2012–2020) of tourist arrivals in Mallorca, precipitation and injected water into the aquifer in Deià. Orange area corresponds to the total number of tourist arrivals to Mallorca per month (IBESTAT, 2023). Blue bars correspond to the accumulated precipitations per month (AEMET, 2022). Green area corresponds to the volume of water injected into the aquifer by the WWTP of Deià (ABAQUA, 2022). Red shadowed areas correspond to the high tourism season and purple lines correspond to the two different samplings of April and August 2019.

the cove, and ^{228}Ra to normalize for mixing.

$$\left[\frac{^{224}Ra}{^{228}Ra}\right]_{end} = \left[\frac{^{224}Ra}{^{228}Ra}\right]_{cw} \cdot e^{-\lambda_{224}\cdot\tau_r} \quad (4)$$

Where, $\left[\frac{^{224}Ra}{^{228}Ra}\right]_{end}$ and $\left[\frac{^{224}Ra}{^{228}Ra}\right]_{cw}$ are the AR between the excess activities of ^{224}Ra and ^{228}Ra (which corresponds to the difference between the coastal water samples and the background concentration at the open ocean (OCN)) in the endmember (as detailed in the next paragraph) and coastal waters, respectively. The τ_r was calculated for April (3.0 ± 0.7 d) but could not be estimated for August due to the relatively short τ_r. Subsequently, we estimated the minimum τ_r (1.5 d) that can be estimated using Ra isotopes when considering the relative average errors associated to the ^{224}Ra and ^{228}Ra ($d^{224}Ra$ and $d^{228}Ra$) in the coastal stations (see Eq. (5)) (Knee et al., 2010), as follows:

$$\tau_r = \frac{ln\left(1 - \sqrt{\left(d^{228}Ra\right)^2 + \left(d^{224}Ra\right)^2}\right)}{-\lambda_{224}} \quad (5)$$

This is the minimum time that can be estimated with Ra isotopes, thus it represents an upper estimate of this temporal scale and we can only infer that the flushing times are <1.5 d in August. Notice that using 1.5 d as an upper estimate of the Ra water age, we produce conservative estimates of SGD (see Eq. (1)). Considering the temporal scales of transport processes for Ra, this short time also suggests that steady-state conditions are a valid assumption for the system (Rodellas et al., 2021).

As derived from the distribution of Ra isotopes and salinity, as well as from visual identification, the main source of groundwater to the cove in August appears to be the karstic spring inflowing at the western part of the cove. Therefore, the sample collected in this spring (LFS) is considered the best representation of the SGD endmember for ^{228}Ra ($^{228}Ra_{SGD}$). However, since the spring discharges below the water surface, the sample collected had a significant mixture with saline water (as derived from its salinity: 28). Thus, the ^{228}Ra concentration in this sample cannot be used to estimate the SGD flow because the signal of Ra was diluted. In order to provide a conservative estimation of SGD, we extrapolated the ^{228}Ra concentration to an effective zero-salinity endmember using a linear regression (Beck et al., 2009; Tamborski et al., 2020). The estimated zero-salinity ^{228}Ra endmember concentration in August is 3500 ± 300 dpm 100 L^{-1}, resulting in a conservative SGD flow of 65 ± 6 m^3 d^{-1}. Normalizing the SGD by the length of the cove mouth (80 m), the estimated SGD flow rate of 3.0 ± 0.3 10^5 m^3 km^{-1} y^{-1} is similar in magnitude to SGD flows in other small coves in the Island of Mallorca (Rodellas et al., 2014; Tovar-Sánchez et al., 2014). SGD flows in April are not reported due to the low ^{228}Ra concentrations that prevent estimating an accurate SGD flow. These low ^{228}Ra concentrations are however indicative of low SGD fluxes in April. It also should be noticed that the SGD flows calculated are only representative of the periods in which samplings have occurred (snap-shot observations) and provide a qualitative comparison between seasons.

4.2. Influence of the wastewater treatment plant on the SGD flows

The higher ^{228}Ra concentrations and the lower salinities in the cove during August in comparison to April, suggest a higher inflow of SGD in summer. The available knowledge on the springs from the area highlights their rapid response to precipitations, with increased water flows lasting only a few days after the precipitation events (Gelabert and Sàbat, 2002). However, this result disagrees with the precipitation regime in the area during the sampling periods, which were comparable during both samplings (Fig. 5). ^{228}Ra excess inventories inside the cove were ~235 % higher in August than in April and thus they cannot be attributed to changes in the natural recharge of the coastal aquifer. This is also consistent with the visual observations of the karstic spring, which was only flowing in August.

Since no other process can explain the increase of SGD in summer, we hypothesize that this difference in magnitude of SGD is likely to be linked with the increase of the wastewater volume injected into the aquifer during summer months (from 4400 m^3 in April to 12,800 m^3 in August), as a consequence of the significant increase in tourism (Fig. 5). Indeed, on the order of ~400 m^3 d^{-1} are injected in the aquifer, on average, every summer day. These large volumes are significantly higher than the SGD fluxes to Cala Deià in August (65 ± 6 m^3 d^{-1}), and thus the increase in injected wastewater volume could support the increase in SGD in summer. We thus suggest that the increase in the demographic pressure in the village during the high tourism season, which results in an increase in the volume of WWTP effluents injected into the aquifer during the high tourism season, may increase the aquifer water table elevation and, therefore, the flow of SGD.

4.3. Nutrient fluxes driven by SGD

SGD inputs might be a relevant source of nutrients to Cala Deià, particularly considering that groundwaters are likely influenced by effluents of the WWTP and that Cala Deià is a small and semi-enclosed system, which may have a limited nutrient flushing. Thus, relatively small nutrient inputs from SGD can have a significant impact on coastal ecology. The SGD-driven nutrient flux can be directly estimated by multiplying the Ra flux supplied by SGD by the nutrient to ^{228}Ra ratio concentration from the SGD endmember (LFS) (Cook et al., 2018; Olid et al., 2022; Santos et al., 2008; Tovar-Sánchez et al., 2014). The estimated SGD-driven nutrient fluxes for DIN, DIP, and DSi are 2.0 ± 0.2 mol m^{-2} y^{-1}, 0.15 ± 0.02 mol m^{-2} y^{-1}, 0.14 ± 0.01 mol m^{-2} y^{-1}, respectively. The calculated SGD-driven DIN fluxes in Cala Deià are comparable with mean global estimates in carbonate coastal systems (1.2 mol m^{-2} y^{-1}; Santos et al., 2021), but they fit in the lower 25 % fluxes estimated for local sites (<1 km^2) and rocky areas. The high DIP fluxes in Cala Deià are up to three times the top-end values reported in other karst aquifers and are similar to the mean values in rocky areas. DIP fluxes supplied by SGD to Cala Deià fit in the higher 75th percentile of total reported cases in Mediterranean sites (Rodellas et al., 2015a). Estimated DSi fluxes are in the lower ranges of the world karst or rocky areas (Santos et al., 2021). Fluxes estimated in Cala Deià are similar or higher to other sites influenced by WWTP or sewage in other locations of the globe (i.e. Bishop et al., 2017; Rodellas et al., 2018; Tamborski et al., 2020).

Besides SGD inputs, there are no other relevant inputs of nutrients into Cala Deià, since no superficial waters were discharging into the cove and the sediment of the cove (mostly composed of stones and coarse-grain sands) is often considered a negligible nutrient source (Lü et al., 2005). Atmospheric deposition could also contribute as a net supplier of nutrients to the cove. However, considering the cove area and mean atmospheric nutrient fluxes in the region (Markaki et al., 2010), it produces atmospheric nutrient fluxes that would be 2 to 3 orders of magnitude lower than SGD-driven nutrient fluxes and thus can be neglected. Since nutrient fluxes supplied by SGD were only estimated for August, a quantitative comparison of nutrient fluxes between seasons cannot be conducted. A semi-quantitative evaluation can be conducted by considering nutrient inventories in the cove for April and August, together with the nutrient inventories that could be attributed to SGD in August (i.e. SGD nutrient inputs multiplied by the flushing time derived from Ra isotopes and the study area) (see Fig. 6). The measured DIN, DIP, and DSi inventories in the cove are much larger in August than in April (3, 10, and 1.5 times higher, respectively), potentially responding to a higher input of nutrients in August compared to April. The nutrient inventories that could be attributed to SGD are comparable in magnitude to the inventories measured in the bay for DIN and DIP, indicating that SGD is most likely the main source of these nutrients. Regarding DSi, SGD could only contribute to 50 % of the DSi inventories observed in the cove, implying that another DSi source is needed to justify the observed inventories. This missing source could be associated with the

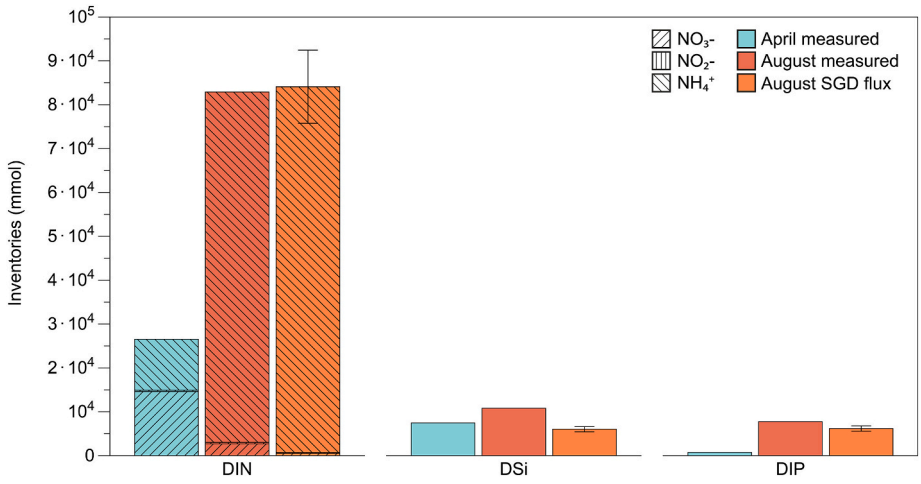

Fig. 6. Dissolved inorganic nutrient inventories during April (blue), August (red) and inventories attributed to SGD (orange). Speciation for DIN is also represented.

constant erosion of the stones and sand of the shore (Tréguer and De La Rocha, 2013), a hypothesis that is consistent with the higher DSi concentrations measured on ST1, 2, and 3.

Focusing on the nitrogen species (Fig. 6), the DIN inventory in the cove is mostly composed of NO_3^- in April (55 %), whilst the main species is NH_4^+ in August (96 %). The contribution of NO_2^- in the total DIN inventories is insignificant during both seasons ($\leq$1 %). Such differences in nitrogen speciation in cove waters can be partially explained by the groundwater sources of these nutrients; in April, most of the N is most likely provided from the subterranean flows from the ephemeral streams, which are enriched in NO_3^-. On the contrary, the most important source of N is the karstic spring, which is mainly composed of NH_4^+ (99 %) most likely because of the water injected from the WWTP, which is also rich in NH_4^+.

Both the seasonal pattern of groundwater discharge (i.e. higher SGD in periods with higher WWTP injection) and the speciation of N in the karstic spring (i.e. DIN mainly composed of NH_4^+) are consistent with wastewaters injected into the coastal aquifers being the main source of N to the Cala Deià via SGD. To better establish the potential origin of the N concentrations in Cala Deià, we used the isotopic signature of N ($\partial^{15}N$). According to the published literature, $\partial^{15}N$ values from WWTP and sewage waters are between +10 and + 22 ‰, between +2 and + 8 ‰ for groundwaters from natural systems, and 1 and 3.8 ‰ for western Mediterranean seawaters (Cole et al., 2005; Kendall et al., 2007; Pantoja et al., 2002). The $\partial^{15}N$ signatures for the karstic spring (LFS; 10.3 ‰) fall within the range of waters impacted by wastewater effluents and sewage waters (Fig. 7), suggesting that the high N loads could be released by the WWTP effluents. This is consistent with the distribution and temporal variability of salinity and Ra concentrations in the cove, as well as with the observed variability of nutrient inventories and N speciation. The relatively high values also observed in cove waters (8.3 ‰ in ST10) reflect the contribution of anthropogenic sources (i.e. WWTP effluents) in the nutrient inventories observed in Cala Deià.

The contribution of natural sources alone cannot explain the large flux of DIP in summer in Cala Deià (0.66 mmol m^{-2} d^{-1}), especially in comparison to other carbonate karstic systems (average SGD fluxes of 0.021 mmol m^{-2} d^{-1}; Santos et al., 2021) where phosphate is removed and easily gets attached to the carbonate surfaces by co-precipitating with dissolved Ca, Al or Fe (Cable et al., 2002; De Jonge and Villerius, 1989; Price et al., 2010; Weiskel and Howes, 1992; Zanini et al., 1998). Considering the large amount of water injected into the aquifer from the WWTP (412 m^3 d^{-1}) and the high DIP concentrations of these effluents (66.3 mmol m^{-3}), the high SGD-driven DIP fluxes are also consistent with the influence of the WWTP injection flux. The primary source of DIP is likely human excreta, soaps, and detergents, as the area lacks significant farms or industries employing fertilizers. Notice that we aimed to establish a connection between injected WWTP effluents, SGD water and nutrient fluxes into Cala Deià, prioritizing proof over precise

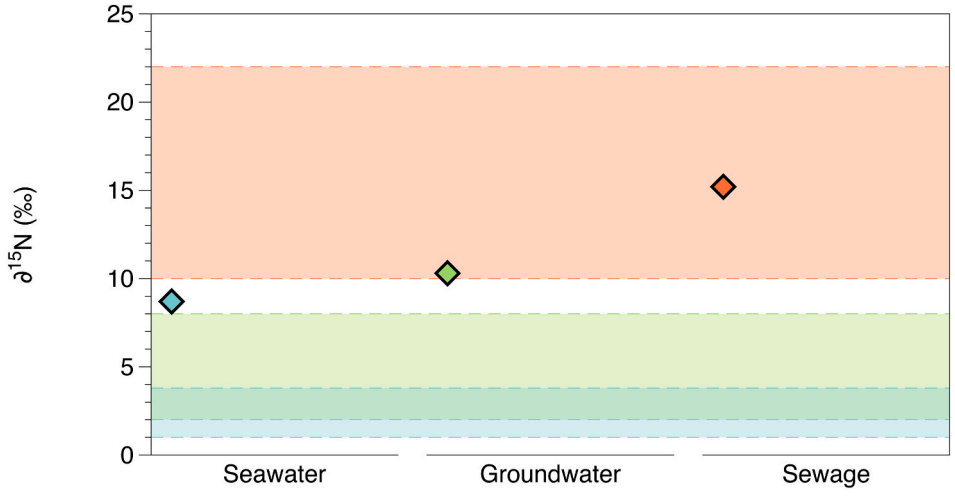

Fig. 7. The $\partial^{15}N$ from Cala Deià in comparison to average values reported in the literature (Cole et al., 2005; Kendall et al., 2007; Pantoja et al., 2002). Blue, green and orange areas correspond to seawater, groundwater and sewage values from the literature. Diamonds correspond to samples measured in Cala Deià.

SGD flow estimations. Acknowledging the semi-quantitative nature of our SGD estimates and the inherent analytical and conceptual uncertainties, our modeling approach consistently opts for conservative estimates, preventing water flow and solute flux overestimations. Despite these considerations, our results unequivocally demonstrate a direct impact of WWTP effluents on the magnitude of SGD and solute inputs in Cala Deià.

4.4. SGD impact on the water quality and coastal ecosystem

4.4.1. Phytoplankton blooms

In Cala Deià, the mean coastal water ratio DIN:DIP in August (31:1) was above the Redfield ratio (16:1), indicating phosphorus as a limiting nutrient. Therefore, inputs of DIP can be particularly relevant to sustain productivity or trigger phytoplankton blooms in Cala Deià (as well as on other coasts of the Illes Balears). The high SGD-driven nutrient fluxes and the relatively low DIN:DIP ratio of discharging groundwaters (5:1 in groundwaters from the karstic spring) can thus play a major role in regulating the important phytoplankton blooms recurrently occurring in the cove during summer months.

In this sense, the concentration of Chl-*a* can be used as an indicator of the risk of eutrophication and thus a degradation of the seawater quality (Colella et al., 2016). According to UN/MAP (2017) the threshold limits for moderate/good coastal water quality for the Mediterranean northwestern islands should be below 1.20 mg Chl-*a* L^{-1}. During August, Chl-*a* concentrations in the closest stations to the shore, which had eutrophic levels, were three times above those limits, with maximum concentrations of ~4 mg Chl-*a* L^{-1}. These high Chl-*a* concentrations are indicative of an algal bloom occurring during the survey. Since the main source of nutrients into the cove is SGD enriched in nutrients due to the injection of WWTP effluents into the aquifer, this mechanism appears to play a significant role in the degradation of the seawater quality according to EU standards (UN/MAP, 2017). It should be noted that episodic blooms during summer had already been detected in Cala Deià (Puigserver et al., 2008) and are not exclusive to this site, but are common in Mediterranean enclosed areas influenced by SGD (Basterretxea et al., 2007). Those blooms are usually dominated by *Alexandrium minutum*, *Dinophysis sacculus*, *Karlodinium* spp. and *Gymnodium* spp. at the shallower areas of the coves (Basterretxea et al., 2018).

4.4.2. Seagrass meadows

The long-term effect of the SGD-driven nutrient inputs to the cove can also be observed in the seagrass present in the cove, which integrates the isotopic signature of the nutrient sources used to support their growth (Andrisoa et al., 2019). *Posidonia oceanica* usually inhabits pristine transparent waters, under oligotrophic conditions and carbonate sediments that confer a P-limited environment (Short, 1987). Through their roots and leaves, *Posidonia oceanica* can incorporate inorganic or organic nutrients present in seawater (Garcias-Bonet et al., 2016; Welsh, 2000). Depending on the main source of nitrogen the seagrass will vary its isotopic ratio ($\partial^{15}N$), presenting low isotopic signatures (<4 ‰; Illes Balears) if the main source is atmospheric (Bedard-Haughn et al., 2003) or higher if nitrogen is mainly sourced by anthropogenic activities (Apostolaki et al., 2012; Fernandes et al., 2009).

The mean value reported in leaves tissues of *Posidonia oceanica* in this study (4.7 ± 1.9 ‰) is relatively high compared to the mean $\partial^{15}N$ signal of 3.7 ± 1.1 ‰ in leaves from the plant in other sites of the Illes Balears (Fourqurean et al., 2007). These relatively high values, together with the maximum $\partial^{15}N$ signature of 7.2 ‰ measured in the site, most likely reflect the relevant contribution of N from anthropogenic sources (i.e. WWTP effluents via SGD). Indeed, the mean value in Cala Deià is similar to the signatures of seagrass meadows in highly pressured areas with emissaries discharging near the seagrass meadows or irrigated coastal areas with WWTP treated waters (Fourqurean et al., 2007; Garcias-Bonet et al., 2016). The maximum in Cala Deià ($\partial^{15}N = 7.2$ ‰) is almost as high as the two maximum values reported in the Illes Balears (7.41 ‰ and 7.54 ‰ in Santa Eulària and Can Picafort, respectively), which correspond to highly impacted areas. Thus, the isotopic signatures in seagrass meadows in Cala Deià are consistent with the influence of anthropogenic nutrient loads delivered to the cove by SGD. In addition to acting as a nutrient source, these SGD-driven nutrient inputs can turn into algal blooms that can affect the transparency of the waters of the cove and/or enrich the sediment with organic matter, enhancing sulfide toxicity and hypoxia, and therefore directly affect the *Posidonia oceanica* ecosystem (Alcoverro et al., 2001; Calleja et al., 2007).

4.5. Water management potential impact on SGD ecosystem services

SGD plays an important role in the provision of Ecosystem Services to coastal societies (Alorda-Kleinglass et al., 2021). The tourism industry benefits from these Ecosystem Services (Apostolopoulos et al., 2002), but the massive development of this industry endangers or even destroys the same Ecosystem Services that it nurtures from. These Ecosystem Services have also been reported to be endangered by high anthropogenic pressure on the beaches of California (Yau et al., 2014) or Hawai'i (Knee et al., 2008), where the transference of pathogens through SGD could endanger the swimmers' health, and therefore their well-being. In addition, cultural Ecosystem Services could also be negatively affected, such as recreational activities or aesthetic values, due to the change of perception that beach users might have from those sites. In this direction, when algal blooms develop in a frequented coastal area due to the input of nutrients from SGD, changes of color can shape the perception of both tourists and local villagers who might decide not to go back, with an ultimate and direct impact on the local economy (Sanseverino et al., 2016). The Cala Deià seems to exemplify such potential changes in users' perception, especially when related to cultural Ecosystem Services. Moreover, the Ecosystem Service provided by the Cala Deià related to developing recreational activities could also be negatively affected, moving from the enjoyment of swimming in clean and pristine waters to the rejection of entering such waters due to their color. Consequently, the same industry that benefits from Ecosystem Services threatens them through the increase of wastewater effluents injected into the aquifer that is subsequently channeled to the cove via SGD.

Whilst this study focuses on a particular cove, the situation occurring in Cala Deià is likely to occur in many other areas along the Mediterranean coast, which is characterized by karstic coastal aquifers (carbonate lithologies account for 46 % of Mediterranean coastlines; (Hartmann and Moosdorf, 2012) and by ranking among the top touristic destinations of the world. In particular, the same situation is also expected to happen in many other sites of the Illes Balears. The four islands from the Illes Balears have 10 WWTP with injection wells into coastal aquifers, all of them located in sensitive touristic areas affected by its important seasonality. Additionally, there are up to 32 WWTPs that discharge into ephemeral streams or lagoons, which can also leach into the aquifer or inflow to the coastal sea. SGD-driven nutrient inputs from WWTP with injection wells not only have an important impact on the coastal ecosystem with the proliferation of phytoplankton blooms that reduce the seawater quality but also on the societies that live there (Wada et al., 2021). Indeed the management of such services is crucial in Mediterranean regions due to the scarcity and high demand of freshwater resources (Erostate et al., 2020).

5. Conclusions

This study highlights the importance of SGD as a pathway delivering anthropogenic nutrients from a coastal aquifer influenced by the injection of wastewater into the coastal sea, and the potential impacts of these inputs on coastal ecosystems and societies. A small cove (Cala Deià) from a Mediterranean touristic area is studied in the present work. The seasonality of touristic pressure directly translates to direct changes in the amount of wastewater treated in the local WWTP and the volume

of effluents injected into the aquifer, which alters the aquifer hydrology. Such alterations are reflected in an increase in the flow of groundwater discharge to a nearby cove and the fluxes of nutrients supplied to the cove. Due to such inputs of SGD-driven nutrients, coastal inventories of DIN and DIP increase by three and one order of magnitude, respectively, in the period of higher touristic pressure, i.e. summer months. These high nutrient fluxes may be contributing to algal blooms at the cove and therefore to the degradation of the quality of seawater. The anthropogenic origin of SGD-driven nutrients can be tracked on the seawaters and seagrass meadows of the cove, with a high $\partial^{15}N$ signature indicative of polluted areas.

Submarine groundwater discharge driven-nutrient inputs have been documented to have important implications for the coastal ocean (Lecher and Mackey, 2018; Santos et al., 2021). This study demonstrates that the large pressure on coastal areas produced by tourism activities can contribute to altering these SGD fluxes, endangering coastal ecosystems and the services they provide. This is particularly relevant for highly touristic areas such as the Illes Balears or the Mediterranean coast. This study presents an opportunity for researchers, managers, and policymakers to better understand and manage coastal areas under high anthropogenic pressure by considering the potential role of SGD.

CRediT authorship contribution statement

Aaron Alorda-Kleinglass: Conceptualization, Funding acquisition, Investigation, Visualization, Writing – original draft, Writing – review & editing. **Valentí Rodellas:** Conceptualization, Investigation, Supervision, Writing – review & editing. **Marc Diego-Feliu:** Conceptualization, Investigation, Writing – review & editing. **Núria Marbà:** Resources, Writing – review & editing. **Carlos Morell:** Investigation, Writing – review & editing. **Jordi Garcia-Orellana:** Conceptualization, Resources, Supervision, Writing – review & editing.

Declaration of competing interest

The authors declare that they have no known competing financial interests or personal relationships that could have appeared to influence the work reported in this paper.

Data availability

Data will be made available on request.

Acknowledgments

This work is dedicated to Jordi Garcia Orellana, a passionate professor, mentor, and friend who devoted his career to inspiring and encouraging many young researchers. The authors acknowledge the financial support of the Spanish Ministry of Science, Innovation and Universities, through the "Maria de Maeztu" programme for Units of Excellence to ICTA (UAB) (CEX2019-000940-M) and IMEDEA (CSIC-UIB) (CEX2021-001198), the Generalitat de Catalunya (MERS; 2021 SGR – 640) and the projects OPAL (PID2019-110311RB-C21). The authors would also like to acknowledge the help and financial support provided by the Foundation Iniciatives del Mediterrani. We would like to thank all the colleagues from the Grup de Recerca en Radioactivitat Ambiental de Barcelona – GRAB (Universitat Autònoma de Barcelona). A. Alorda-Kleinglass acknowledges financial support from ICTA "Unit of Excellence" (MinECo, MDM2015-0552-17-1) and PhD fellowship, BES-2017-080740. V. Rodellas acknowledges financial support from the Beatriu de Pinós postdoctoral program of the Generalitat de Catalunya autonomous government (2019-BP-00241). M. Diego-Feliu acknowledges the economic support from the FI-2017 fellowships of the Generalitat de Catalunya autonomous government (2017FI_B_00365). N. Marbà acknowledges financial support from the Government of the Balearic Islands (project PRD2018/18). We would also like to thank ABAQUA for providing the data of the WWTP and allowing us to take samples from their installations. The authors thank the comments and revisions done by Dr. Isabel Ruiz-Mallen.

Appendix A. Supplementary data

Supplementary data to this article can be found online at https://doi.org/10.1016/j.scitotenv.2024.170940.

References

ABAQUA, 2022. Portal de l'Agència Balear de l'Aigua i la Qualitat Ambiental [WWW Document]. URL. https://abaqua.cat/es/seccio/producio-y-captacio-daigua/.

Adyasari, D., Hassenrück, C., Oehler, T., Sabdaningsih, A., Moosdorf, N., 2019. Microbial community structure associated with submarine groundwater discharge in northern Java (Indonesia). Sci. Total Environ. 689, 590–601. https://doi.org/10.1016/j.scitotenv.2019.06.193.

AEMET, 2022. Base de datos meteorológica. Gráficos-Datos Extremos-Datos diarios de Temperatura [WWW Document]. URL https://datosclima.es/Aemet2013/Precipitastad2013.php (accessed 7.10.17).

Alcoverro, T., Cerbiän, E., Ballesteros, E., 2001. The photosynthetic capacity of the seagrass Posidonia oceanica: influence of nitrogen and light. J. Exp. Mar. Biol. Ecol. 261, 107–120.

Alorda-Kleinglass, A., Ruiz-Mallén, I., Diego-Feliu, M., Rodellas, V., Bruach-Menchén, J. M., Garcia-Orellana, J., 2021. The social implications of submarine groundwater discharge from an ecosystem services perspective: a systematic review. Earth-Science Rev. 221, 103742 https://doi.org/10.1016/j.earscirev.2021.103742.

Amato, D.W., Bishop, J.M., Glenn, C.R., Dulai, H., Smith, C.M., 2016. Impact of submarine groundwater discharge on marine water quality and reef biota of Maui. PLoS One 11, 1–28. https://doi.org/10.1371/journal.pone.0165825.

Amato, D.W., Whittier, R.B., Dulai, H., Smith, C.M., 2020. Algal bioassays detect modeled loading of wastewater-derived nitrogen in coastal waters of O'ahu, Hawai'i. Mar. Pollut. Bull. 150, 110668.

Andrisoa, A., Stieglitz, T.C., Rodellas, V., Raimbault, P., 2019. Primary production in coastal lagoons supported by groundwater discharge and porewater fluxes inferred from nitrogen and carbon isotope signatures. Mar. Chem. 210, 48–60. https://doi.org/10.1016/j.marchem.2019.03.003.

Apostolaki, E.T., Vizzini, S., Karakassis, I., 2012. Leaf vs. epiphyte nitrogen uptake in a nutrient enriched Mediterranean seagrass (Posidonia oceanica) meadow. Aquat. Bot. 96, 58–62. https://doi.org/10.1016/j.aquabot.2011.09.008.

Apostolopoulos, Yiorgos, Apostolopoulos, Yorghos, Gayle, D.J., 2002. Island Tourism and Sustainable Development: Caribbean, Pacific, and Mediterranean Experiences. Greenwood Publishing Group.

Basterretxea, G., Garcés, E., Jordi, A., Anglès, S., Masó, M., 2007. Modulation of nearshore harmful algal blooms by in situ growth rate and water renewal. Mar. Ecol. Prog. Ser. 352, 53–65. https://doi.org/10.3354/meps07168.

Basterretxea, G., Tovar-Sánchez, A., Beck, A.J., Masqué, P., Bokuniewicz, H.J., Coffey, R., Duarte, C.M., Garcia-Orellana, J., Garcia-Solsona, E., Martinez-Ribes, L., Vaquer-Sunyer, R., 2010. Submarine groundwater discharge to the coastal environment of a Mediterranean island (Majorca, Spain): ecosystem and biogeochemical significance. Ecosystems 13, 629–643. https://doi.org/10.1007/s10021-010-9334-5.

Basterretxea, G., Torres-Serra, F.J., Alacid, E., Anglès, S., Camp, J., Ferrera, I., Flo, E., Font-Muñoz, J.S., Jordi, A., Reñé, A., Salgado-Hernanz, P.M., Sampedro, N., Garcés, E., 2018. Cross-shore environmental gradients in the Western Mediterranean coast and their influence on nearshore phytoplankton communities. Front. Mar. Sci. 5, 1–13. https://doi.org/10.3389/fmars.2018.00078.

Beck, A.J., Rapaglia, J.P., Cochran, J.K., Bokuniewicz, H., 2007. Radium mass-balance in Jamaica Bay, NY: evidence for a substantial flux of submarine groundwater. Mar. Chem. 106, 419–441. https://doi.org/10.1016/j.marchem.2007.03.008.

Beck, A.J., Cochran, J.K., Sañudo-Wilhelmy, S.A., 2009. Temporal trends of dissolved trace metals in Jamaica Bay, NY: importance of wastewater input and submarine groundwater discharge in an urban estuary. Estuar. Coasts 32, 535–550. https://doi.org/10.1007/s12237-009-9140-5.

Bedard-Haughn, A., Van Groenigen, J.W., Van Kessel, C., 2003. Tracing 15N through landscapes: potential uses and precautions. J. Hydrol. 272, 175–190.

Bishop, J.M., Glenn, C.R., Amato, D.W., Dulai, H., 2017. Effect of land use and groundwater flow path on submarine groundwater discharge nutrient flux. J. Hydrol. Reg. Stud. 11, 194–218. https://doi.org/10.1016/j.ejrh.2015.10.008.

Boehm, A.B., Shellenbarger, G.G., Paytan, A., 2004. Groundwater discharge: potential association with fecal indicator bacteria in the surf zone. Environ. Sci. Technol. 38, 3558–3566. https://doi.org/10.1021/es035385a.

Cable, J.E., Corbett, D.R., Walsh, M.M., 2002. Phosphate uptake in coastal limestone aquifers: a fresh look at wastewater management. Limnol. Oceanogr. Bull. 11, 29–32. https://doi.org/10.1002/lob.200211229.

Calleja, M.L., Marbà, N., Duarte, C.M., 2007. The relationship between seagrass (Posidonia oceanica) decline and sulfide porewater concentration in carbonate sediments. Estuar. Coast. Shelf Sci. 73, 583–588. https://doi.org/10.1016/j.ecss.2007.02.016.

Cole, M.L., Kroeger, K.D., McClelland, J.W., Valiela, I., 2005. Macrophytes as indicators of land-derived wastewater: application of a δ15N method in aquatic systems. Water Resour. Res. 41, 1–9. https://doi.org/10.1029/2004WR003269.

Colella, S., Falcini, F., Rinaldi, E., Sammartino, M., Santoleri, R., 2016. Mediterranean ocean colour chlorophyll trends. PLoS One 11, 1–16. https://doi.org/10.1371/journal.pone.0155756.
Cook, P.G., Rodellas, V., Stieglitz, T.C., 2018. Quantifying surface water, Porewater and groundwater interactions using tracers: tracer fluxes, water fluxes and endmember concentrations. Water Resour. Res. 1–14 https://doi.org/10.1002/2017WR021780.
Croes, R., 2013. Tourism specialization and economic output in small islands. Tour. Rev. 68, 34–48. https://doi.org/10.1108/TR-09-2013-0050.
Dailer, M.L., Knox, R.S., Smith, J.E., Napier, M., Smith, C.M., 2010. Using δ15N values in algal tissue to map locations and potential sources of anthropogenic nutrient inputs on the island of Maui, Hawai'i, USA. Mar. Pollut. Bull. 60, 655–671. https://doi.org/10.1016/j.marpolbul.2009.12.021.
Dailer, M.L., Ramey, H.L., Saephan, S., Smith, C.M., 2012. Algal δ 15N values detect a wastewater effluent plume in nearshore and offshore surface waters and three-dimensionally model the plume across a coral reef on Maui, Hawai'i, USA. Mar. Pollut. Bull. 64, 207–213. https://doi.org/10.1016/j.marpolbul.2011.12.004.
De Jonge, V.N., Villerius, L.A., 1989. Possible role of carbonate dissolution in estuarine phosphate dynamics. Limnol. Oceanogr. 34, 332–340.
Deyà Tortella, B., Tirado, D., 2011. Hotel water consumption at a seasonal mass tourist destination. The case of the island of Mallorca. J. Environ. Manag. 92, 2568–2579. https://doi.org/10.1016/j.jenvman.2011.05.024.
Diego-Feliu, M., Rodellas, V., Alorda-Kleinglass, A., Tamborski, J., van Beek, P., Heins, L., Bruach, J.M., Arnold, R., Garcia-Orellana, J., 2020. Guidelines and limits for the quantification of Ra isotopes and related radionuclides with the radium delayed coincidence counter (RaDeCC). J. Geophys. Res. Ocean. 125, e2019JC015544 https://doi.org/10.1029/2019jc015544.
Diego-Feliu, M., Rodellas, V., Saaltink, M.W., Alorda-Kleinglass, A., Goyetche, T., Martínez-Pérez, L., Folch, A., Garcia-Orellana, J., 2021. New perspectives on the use of 224Ra/228Ra and 222Rn/226Ra activity ratios in groundwater studies. J. Hydrol. 596 https://doi.org/10.1016/j.jhydrol.2021.126043.
Diego-Feliu, M., Rodellas, V., Alorda-Kleinglass, A., Saaltink, M., Folch, A., Garcia-Orellana, J., 2022. Extreme precipitation events induce high fluxes of groundwater and associated nutrients to the coastal ocean. Hydrol. Earth Syst. Sci. Discuss. 2022, 1–27. https://doi.org/10.5194/hess-26-4619-2022.
Dulai, H., Kleven, A., Ruttenberg, K., Briggs, R., Thomas, F., 2016. Emerging issues in groundwater resources. In: Fares, A. (Ed.), Emerging Issues in Groundwater Resources. Springer International, pp. 187–221. https://doi.org/10.1007/978-3-319-32008-3.
Dulai, H., Smith, C.M., Amato, D.W., Gibson, V., Bremer, L.L., 2023. Risk to native marine macroalgae from land-use and climate change-related modifications to groundwater discharge in Hawai'i. Limnol. Oceanogr. Lett. 8, 141–153. https://doi.org/10.1002/lol2.10232.
EEA, 2019. Urban Waste Water Treatment for 21st Century Challenges. https://doi.org/10.2800/362039.
Erostate, M., Huneau, F., Garel, E., Ghiotti, S., Vystavna, Y., Garrido, M., Pasqualini, V., 2020. Groundwater dependent ecosystems in coastal Mediterranean regions: characterization, challenges and management for their protection. Water Res. 172, 115461 https://doi.org/10.1016/j.watres.2019.115461.
Fackrell, J.K., Glenn, C.R., Popp, B.N., Whittier, R.B., Dulai, H., 2016. Wastewater injection, aquifer biogeochemical reactions, and resultant groundwater N fluxes to coastal waters: Kā'anapali, Maui, Hawai'i. Mar. Pollut. Bull. 110, 281–292. https://doi.org/10.1016/j.marpolbul.2016.06.050.
Fernandes, M., Bryars, S., Mount, G., Miller, D., 2009. Seagrasses as a sink for wastewater nitrogen: the case of the Adelaide metropolitan coast. Mar. Pollut. Bull. 58, 303–308.
Fourqurean, J.W., Marbà, N., Duarte, C.M., Diaz-Almela, E., Ruiz-Halpern, S., 2007. Spatial and temporal variation in the elemental and stable isotopic content of the seagrasses Posidonia oceanica and Cymodocea nodosa from the Illes Balears, Spain. Mar. Biol. 151, 219–232. https://doi.org/10.1007/s00227-006-0473-3.
Garcés, E., Basterretxea, G., Tovar-Sánchez, A., 2011. Changes in microbial communities in response to submarine groundwater input. Mar. Ecol. Prog. Ser. 438, 47–58. https://doi.org/10.3354/meps09311.
Garcia, C., Deyà-Tortella, B., Lorenzo-Lacruz, J., Morán-Tejeda, E., Rodríguez-Lozano, P., Tirado, D., 2022. Zero tourism due to COVID-19: an opportunity to assess water consumption associated to tourism. J. Sustain. Tour. 0, 1–16. https://doi.org/10.1080/09669582.2022.2079652.
Garcia-Orellana, J., Cochran, J.K., Bokuniewicz, H., Daniel, J.W.R., Rodellas, V., Heilbrun, C., 2014. Evaluation of 224Ra as a tracer for submarine groundwater discharge in Long Island Sound (NY). Geochim. Cosmochim. Acta 141, 314–330. https://doi.org/10.1016/j.gca.2014.05.009.
Garcia-Orellana, J., Rodellas, V., Tamborski, J., Diego-Feliu, M., Van Beek, P., Weinstein, Y., Charette, M.A., Alorda-Kleinglass, A., Michael, H.A., Stieglitz, T.C., Scholten, J.C., 2021. Radium isotopes as submarine groundwater discharge (SGD) tracers: review and recommendations. Earth Sci. Rev. https://doi.org/10.1016/j.earscirev.2021.103681.
Garcias-Bonet, N., Arrieta, J.M., Duarte, C.M., Marbà, N., 2016. Nitrogen-fixing bacteria in Mediterranean seagrass (Posidonia oceanica) roots. Aquat. Bot. 131, 57–60. https://doi.org/10.1016/j.aquabot.2016.03.002.
Garcia-Solsona, E., Garcia-Orellana, J., Masqué, P., Dulaiova, H., 2008. Uncertainties associated with 223Ra and 224Ra measurements in water via a delayed coincidence counter (RaDeCC). Mar. Chem. 109, 198–219. https://doi.org/10.1016/j.marchem.2007.11.006.
Garcia-Solsona, E., Garcia-Orellana, J., Masqué, P., Garcés, E., Radakovitch, O., Mayer, A., Estradé, S., Basterretxea, G., 2010. An assessment of karstic submarine groundwater and associated nutrient discharge to a Mediterranean coastal area (Balearic Islands, Spain) using radium isotopes. Biogeochemistry 97, 211–229. https://doi.org/10.1007/s10533-009-9368-y.
Gelabert, B., Sàbat, F., 2002. Relationchips between groundwater and geological structure in the Sierra de Tramuntana of Mallorca (Balearic Islands). Geogaceta 31, 107–110.
Giménez, J., Barón, A., Comas, M., González, C., 2014. Hidrogeologia de les Illes Balears: Característiques càrstics dels aqüífers. Endins 36, 9–26.
Glenn, C., Whittier, R., Dailer, M.L., Dulai, H., El-Kadi, A., Fackrell, J.K., Kelly, J., Waters, C., Sevadjian, J., 2013. Lahaina Groundwater Tracer Study Lahaina, Maui, Hawai'i. Final Report, EPA Rep, p. 502.
GOIB, 2022. Portal de l'Aigua de les Illes Balears-Consums d'aigua [WWW Document]. RESUM Anu. DADES D'ABASTIMENT URBÀ D'AIGUA, anys 2000 a 2021 SUBMINISTRAMENT I Consum Anu. PER TERME Munic. – MALLORCA. URL. https://www.caib.es/sites/aigua/ca/consum_aigua/.
GOIB-Observatori del treball, 2021. Observatori del treball-Deià [WWW Document]. URL. http://www.caib.es/sites/observatorideltreball/ca/deia-26989/ (accessed 10.14.21).
Govern de les Illes Balears, 2014. Masas de agua subterránea de Baleares. Deià-Valldemossa - 1802M3, Palma.
Grasshoff, P., 1983. Methods of seawater analysis. Verlag Chem. FRG 419, 61–72.
Gutiérrez-Martín, D., Gil-Solsona, R., Saaltink, M.W., Rodellas, V., López-Serna, R., Folch, A., Carrera, J., Gago-Ferrero, P., 2023. Chemicals of emerging concern in coastal aquifers: assessment along the land-ocean interface. J. Hazard. Mater. 448 https://doi.org/10.1016/j.jhazmat.2023.130876.
Hartmann, J., Moosdorf, N., 2012. The new global lithological map database GLiM: a representation of rock properties at the Earth surface. Geochem. Geophys. Geosyst. 13, 1–37. https://doi.org/10.1029/2012GC004370.
Hernández-Terrones, L.M., Null, K.A., Ortega-Camacho, D., Paytan, A., 2015. Water quality assessment in the Mexican Caribbean: impacts on the coastal ecosystem. Cont. Shelf Res. 102, 62–72. https://doi.org/10.1016/j.csr.2015.04.015.
Hosono, T., Ono, M., Burnett, W.C., Tokunaga, T., Taniguchi, M., Akimichi, T., 2012. Spatial distribution of submarine groundwater discharge and associated nutrients within a local coastal area. Environ. Sci. Technol. 46, 5319–5326. https://doi.org/10.1021/es2043867.
IBESTAT, 2022. Datos estadísticos: Economía: Turismo: Alojamientos turísticos: Alojamientos turísticos por isla y municipio, tipo y categoría y año. [WWW Document]. URL. https://www.caib.es/ibestat/estadistiques/06f4cf63-e3a8-4d01-bf9a-32dd529b96b9/1b7fa42e-fef0-43ef-ab5f-cbb2b0e3e972/es/U208009_0002.px (accessed 12.8.22).
IBESTAT, 2023. Datos estadísticos: Economía: Turismo [WWW Document]. URL. https://ibestat.caib.es/ibestat/estadistiques/economia/turisme/0b70b294-81e0-413a-b7b2-3cc3a33593a8 (accessed 12.20.23).
INE, 2022. Viviendas turísticas, plazas y plazas por vivienda turística. Municipios(39363) [WWW Document]. URL. https://www.ine.es/jaxiT3/Datos.htm?t=39363 (accessed 12.8.22).
Johannes, R.E., Hearn, C.J., 1985. The effect of submarine groundwater discharge on nutrient and salinity regimes in a coastal lagoon off Perth. Western Australia. Estuar. Coast. Shelf Sci. 21, 789–800. https://doi.org/10.1016/0272-7714(85)90073-3.
Kantún-Manzano, C.A., Herrera-Silveira, J.A., Arcega-Cabrera, F., 2018. Influence of coastal submarine groundwater discharges on seagrass communities in a subtropical karstic environment. Bull. Environ. Contam. Toxicol. 100, 176–183. https://doi.org/10.1007/s00128-017-2259-3.
Kendall, C., Elliott, E.M., Wankel, S.D., 2007. Tracing anthropogenic inputs of nitrogen to ecosystems. Stable Isot. Ecol. Environ. Sci. Second Ed. 375–449. https://doi.org/10.1002/9780470691854.ch12.
Knee, K.L., Layton, B.A., Street, J.H., Boehm, A.B., Paytan, A., 2008. Sources of nutrients and fecal indicator bacteria to nearshore waters on the north shore of Kaua'i (Hawai'i, USA). Estuar. Coasts 31, 607–622. https://doi.org/10.1007/s12237-008-9055-6.
Knee, K.L., Street, J.H., Grossman, E.E., Boehm, A.B., Paytan, A., 2010. Nutrient inputs to the coastal ocean from submarine groundwater discharge in a groundwater-dominated system: relation to land use (Kona coast, Hawaii, USA). Limnol. Oceanogr. 55, 1105–1122. https://doi.org/10.4319/lo.2010.55.3.1105.
Lapointe, B.E., O'Connell, J.D., Garrett, G.S., 1990. Nutrient couplings between on-site sewage disposal systems, groundwaters, and nearshore surface waters of the Florida Keys. Biogeochemistry 10, 289–307. https://doi.org/10.1007/BF00003149.
Lecher, A.L., Mackey, K.R.M., 2018. Synthesizing the effects of submarine groundwater discharge on marine biota. Hydrology 5, 1–21. https://doi.org/10.3390/hydrology5040060.
Lü, X., Song, J., Li, X., Yuan, H., Zhan, T., Li, N., Gao, X., 2005. Geochemical characteristics of nitrogen in the southern Yellow Sea surface sediments. J. Mar. Syst. 56, 17–27. https://doi.org/10.1016/j.jmarsys.2004.06.009.
Luek, J.L., Beck, A.J., 2014. Radium budget of the York River estuary (VA, USA) dominated by submarine groundwater discharge with a seasonally variable groundwater end-member. Mar. Chem. 165, 55–65. https://doi.org/10.1016/j.marchem.2014.08.001.
Machado, D.A., Imberger, J., 2014. Modeling the impact of natural and anthropogenic nutrient sources on phytoplankton dynamics in a shallow coastal domain, Western Australia. Environ. Fluid Mech. 14, 87–111. https://doi.org/10.1007/s10652-013-9296-1.
Manera, C., Badal, F.N., Bonnail, M., 2018. La indústria invisible, 1950–2016: el desenvolupament del turisme a l'economia de Balears. Lleonard Muntaner, Palma.
Markaki, Z., Loÿe-Pilot, M.D., Violaki, K., Benyahya, L., Mihalopoulos, N., 2010. Variability of atmospheric deposition of dissolved nitrogen and phosphorus in the Mediterranean and possible link to the anomalous seawater N/P ratio. Mar. Chem. 120, 187–194. https://doi.org/10.1016/j.marchem.2008.10.005.
McKenzie, T., Holloway, C., Dulai, H., Tucker, J.P., Sugimoto, R., Nakajima, T., Harada, K., Santos, I.R., 2020. Submarine groundwater discharge: a previously

undocumented source of contaminants of emerging concern to the coastal ocean (Sydney, Australia). Mar. Pollut. Bull. 160, 111519 https://doi.org/10.1016/j.marpolbul.2020.111519.
Michael, H.A., Charette, M.A., Harvey, C.F., 2011. Patterns and variability of groundwater flow and radium activity at the coast: a case study from Waquoit Bay, Massachusetts. Mar. Chem. 127, 100–114. https://doi.org/10.1016/j.marchem.2011.08.001.
Moore, W.S., 2000. Determining coastal mixing rates using radium isotopes. Cont. Shelf Res. 20, 1993–2007. https://doi.org/10.1016/S0278-4343(00)00054-6.
Moore, W.S., Arnold, R., 1996. Measurement of 223Ra and 224Ra in coastal waters using a delayed coincidence counter. J. Geophys. Res. 101, 1321–1329.
Moore, W.S., Reid, D.F., 1973. Extraction of radium from natural waters using manganese-impregnated acrylic fibers. J. Geophys. Res. 78, 8880–8886. https://doi.org/10.1029/JC078i036p08880.
Moosdorf, N., Oehler, T., 2017. Societal use of fresh submarine groundwater discharge: an overlooked water resource. Earth Sci. Rev. 171, 338–348. https://doi.org/10.1016/j.earscirev.2017.06.006.
Olid, C., Rodellas, V., Rocher-Ros, G., Garcia-Orellana, J., Diego-Feliu, M., Alorda-Kleinglass, A., Bastviken, D., Karlsson, J., 2022. Groundwater discharge as a driver of methane emissions from Arctic lakes. Nat. Commun. 13, 1–9. https://doi.org/10.1038/s41467-022-31219-1.
Onac, B.P., Fornós, J.J., Ginés, À., Ginés, J., 2005. Mineralogical Reconnaisance of Caves From Mallorca Island. Endins: publicació d'espeleologia, pp. 131–140.
Orhon, D., Sözen, S., Görgün, E., Ubay Çokgör, E., Artan, N., 1999. Technological aspects of wastewater management in coastal tourist areas. Water Sci. Technol. 39, 177–184. https://doi.org/10.1016/S0273-1223(99)00200-0.
Pantoja, S., Repeta, D.J., Sachs, J.P., Sigman, D.M., 2002. Stable isotope constraints on the nitrogen cycle of the Mediterranean Sea water column. Deep. Res. Part I Oceanogr. Res. Pap. 49, 1609–1621. https://doi.org/10.1016/S0967-0637(02)00066-3.
Price, R.M., Savabi, M.R., Jolicoeur, J.L., Roy, S., 2010. Adsorption and desorption of phosphate on limestone in experiments simulating seawater intrusion. Appl. Geochem. 25, 1085–1091. https://doi.org/10.1016/j.apgeochem.2010.04.013.
Prouty, N.G., Cohen, A., Yates, K.K., Storlazzi, C.D., Swarzenski, P.W., White, D., 2017. Vulnerability of coral reefs to bioerosion from land-based sources of pollution. J. Geophys. Res. Ocean. 122, 9319–9331. https://doi.org/10.1002/2017JC013264.
Puigserver, M., Monerris, N., Moya, G., 2008. Estudi del fitoplàncton de les aigües costaneres de les Illes Balears (2005-2006) en el marc de la implantació de la Directiva Marc Europea de l'Aigua per a l'avaluació del seu estat ecològic. Bolleti la Soc. d'Historia Nat. les Balear. 51, 49–61.
Pujol, L.G., Orfila, A., Ellacuría, A.Á., 2017. Evolución y dinámica de una playa encajada de bloques y gravas en la costa NO de Mallorca (Cala Deià, Mallorca). Geotemas (Madrid) 111–114.
PUMO, 1990. Unidades hidrogeoló gicas de la España peninsular e Islas Baleares. Inf. y Estud.
Rodellas, V., Garcia-Orellana, J., Tovar-Sánchez, A., Basterretxea, G., López-Garcia, J.M., Sánchez-Quiles, D., Garcia-Solsona, E., Masqué, P., 2014. Submarine groundwater discharge as a source of nutrients and trace metals in a Mediterranean bay (Palma Beach, Balearic Islands). Mar. Chem. 160, 56–66. https://doi.org/10.1016/j.marchem.2014.01.007.
Rodellas, V., Garcia-Orellana, J., Masqué, P., Feldman, M., Weinstein, Y., 2015a. Submarine groundwater discharge as a major source of nutrients to the Mediterranean Sea. Proc. Natl. Acad. Sci. U. S. A. 112, 3926–3930. https://doi.org/10.1073/pnas.1419049112.
Rodellas, V., Garcia-Orellana, J., Masqué, P., Font-Muñoz, J.S., 2015b. The influence of sediment sources on radium-derived estimates of submarine groundwater discharge. Mar. Chem. 171, 107–117. https://doi.org/10.1016/j.marchem.2015.02.010.
Rodellas, V., Garcia-Orellana, J., Trezzi, G., Masqué, P., Stieglitz, T.C., Bokuniewicz, H., Cochran, J.K., Berdalet, E., 2017. Using the radium quartet to quantify submarine groundwater discharge and porewater exchange. Geochim. Cosmochim. Acta 196, 58–73. https://doi.org/10.1016/j.gca.2016.09.016.
Rodellas, V., Stieglitz, T.C., Andrisoa, A., Cook, P.G., Raimbault, P., Tamborski, J., van Beek, P., Radakovitch, O., 2018. Groundwater-driven nutrient inputs to coastal lagoons: the relevance of lagoon water recirculation as a conveyor of dissolved nutrients. Sci. Total Environ. 642, 764–780. https://doi.org/10.1016/j.scitotenv.2018.06.095.
Rodellas, V., Stieglitz, T.C., Tamborski, J., van Beek, P., Andrisoa, A., Cook, P.G., 2021. Conceptual uncertainties in groundwater and porewater fluxes estimated by radon and radium mass balances. Limnol. Oceanogr. 1–19 https://doi.org/10.1002/lno.11678.
Sanseverino, I., Conduto, D., Pozzoli, L., Dobricic, S., Lettieri, T., 2016. Algal Bloom and Its Economic Impact. https://doi.org/10.2788/660478.
Santos, I.R., Chen, X., Lecher, A.L., Sawyer, A.H., Moosdorf, N., Rodellas, V., Tamborski, J., Cho, H.-M., Dimova, N., Sugimoto, R., Bonaglia, S., Li, H., Hajati, M.-C., Li, L., 2021. Submarine groundwater discharge impacts on coastal nutrient biogeochemistry. Nat. Rev. Earth Environ. https://doi.org/10.1038/s43017-021-00152-0, 0123456789.
Santos, I.R.S., Burnett, W.C., Chanton, J., Mwashote, B., Suryaputra, I.G.N.A., Dittmar, T., 2008. Nutrient biogeochemistry in a Gulf of Mexico subterranean estuary and groundwater-derived fluxes to the coastal ocean. Limnol. Oceanogr. 53, 705–718.
Sun, Y., Torgersen, T., 1998. The effects of water content and Mn-fiber surface conditions on ^{224}Ra measurement by ^{220}Rn emanation. Mar. Chem. 62, 299–306. https://doi.org/10.1016/S0304-4203(98)00019-X.
Short, F.T., 1987. Effects of sediment nutrients on seagrasses: literature review and mesocosm experiment. Aquat. Bot. 27, 41–57.
Swarzenski, P.W., Dulai, H., Kroeger, K.D., Smith, C.G., Dimova, N., Storlazzi, C.D., Prouty, N.G., Gingerich, S.B., Glenn, C.R., 2016. Observations of nearshore groundwater discharge: Kahekili Beach park submarine springs, Maui, Hawaii. J. Hydrol. Reg. Stud. 11, 147–165. https://doi.org/10.1016/j.ejrh.2015.12.056.
Tamborski, J., van Beek, P., Conan, P., Pujo-Pay, M., Odobel, C., Ghiglione, J.F., Seidel, J.L., Arfib, B., Diego-Feliu, M., Garcia-Orellana, J., Szafran, A., Souhaut, M., 2020. Submarine karstic springs as a source of nutrients and bioactive trace metals for the oligotrophic Northwest Mediterranean Sea. Sci. Total Environ. 732, 1–14. https://doi.org/10.1016/j.scitotenv.2020.139106.
Taniguchi, M., Dulai, H., Burnett, K.M., Santos, I.R., Sugimoto, R., Stieglitz, T.C., Kim, G., Moosdorf, N., Burnett, W.C., 2019. Submarine groundwater discharge: updates on its measurement techniques, geophysical drivers, magnitudes, and effects. Front. Environ. Sci. 7, 1–26. https://doi.org/10.3389/fenvs.2019.00141.
Tovar-Sánchez, A., Basterretxea, G., Rodellas, V., Sánchez-Quiles, D., Garcia-Orellana, J., Masqué, P., Jordi, A., López, J.M., Garcia-Solsona, E., 2014. Contribution of groundwater discharge to the coastal dissolved nutrients and trace metal concentrations in Majorca Island: karstic vs detrital systems. Environ. Sci. Technol. 48, 11819–11827. https://doi.org/10.1021/es502958t.
Tréguer, P.J., De La Rocha, C.L., 2013. The world ocean silica cycle. Annu. Rev. Mar. Sci. 5, 477–501. https://doi.org/10.1146/annurev-marine-121211-172346.
UN/MAP, 2017. Mediterranean Quality Status Report. Mediterr, Action Plan Barcelona Conv, p. 539.
Wada, C.A., Burnett, K.M., Okuhata, B.K., Delevaux, J.M.S., Dulai, H., El-Kadi, A.I., Gibson, V., Smith, C., Bremer, L.L., 2021. Identifying wastewater management tradeoffs: costs, nearshore water quality, and implications for marine coastal ecosystems in Kona, Hawai'i. PLoS One 16, e0257125. https://doi.org/10.1371/journal.pone.0257125.
Weiskel, P.K., Howes, B.L., 1992. Differential transport of sewage-derived nitrogen and phosphorus through a coastal watershed. Environ. Sci. Technol. 26, 352–360.
Welch, E.M., Dulai, H., El-Kadi, A., Shuler, C.K., 2019. Submarine groundwater discharge and stream baseflow sustain pesticide and nutrient fluxes in Faga'alu Bay, American Samoa. Front. Environ. Sci. 7 https://doi.org/10.3389/fenvs.2019.00162.
Welsh, D.T., 2000. Nitrogen fixation in seagrass meadows: regulation, plant–bacteria interactions and significance to primary productivity. Ecol. Lett. 3, 58–71.
Yau, V.M., Schiff, K.C., Arnold, B.F., Griffith, J.F., Gruber, J.S., Wright, C.C., Wade, T.J., Burns, S., Hayes, J.M., McGee, C., Gold, M., Cao, Y., Boehm, A.B., Weisberg, S.B., Colford, J.M., 2014. Effect of submarine groundwater discharge on bacterial indicators and swimmer health at Avalon Beach, CA, USA. Water Res. 59, 23–36. https://doi.org/10.1016/j.watres.2014.03.050.
Yoshioka, R.M., Kim, C.J.S., Tracy, A.M., Most, R., Harvell, C.D., 2016. Linking sewage pollution and water quality to spatial patterns of Porites lobata growth anomalies in Puako, Hawaii. Mar. Pollut. Bull. 104, 313–321. https://doi.org/10.1016/j.marpolbul.2016.01.002.
Zanini, L., Robertson, W.D., Ptacek, C.J., Schiff, S.L., Mayer, T., 1998. Phosphorus characterization in sediments impacted by septic effluent at four sites in central Canada. J. Contam. Hydrol. 33, 405–429.
Zhang, L., Altabet, M.A., Wu, T., Hadas, O., 2007. Sensitive measurement of NH4+15N/14N (δ15NH4+) at natural abundance levels in fresh and saltwaters. Anal. Chem. 79, 5297–5303. https://doi.org/10.1021/ac070106d.